Author Manuscript

Author Manuscript

Author Manuscript

Author Manuscript

HHS Public Access

Author manuscript

Circulation. Author manuscript; available in PMC 2024 January 31.

Published in final edited form as:

Circulation. 2023 January 31; 147(5): 388–408. doi:10.1161/CIRCULATIONAHA.122.059062.

Macrophage derived 25-hydroxycholesterol promotes vascular inflammation, atherogenesis and lesion remodeling

Alberto Canfrán-Duque, PhD[1,2,3], **Noemi Rotllan, PhD**[1,2,3], **Xinbo Zhang, PhD**[1,2,3], **Irene Andrés-Blasco, PhD**[3,4], **Bonne M Thompson, PhD**[5], **Jonathan Sun, BS**[1,2,12], **Nathan L Price, PhD**[1,2,3], **Marta Fernández-Fuertes, BS**[1,2,3], **Joseph W. Fowler, PhD**[1,6], **Diego Gómez-Coronado, PhD**[7], **William C. Sessa, PhD**[1,6], **Chiara Giannarelli, MD, PhD**[8,9], **Robert J Schneider, PhD**[10], **George Tellides, MD, PhD**[1,11], **Jeffrey G McDonald, PhD**[5], **Carlos Fernández-Hernando, PhD**[1,2,3,12], **Yajaira Suárez, PhD**[1,2,3,12]

[1]Vascular Biology and Therapeutics Program, Yale University School of Medicine, New Haven, Connecticut, USA.

[2]Yale Center for Molecular and System Metabolism, Yale University School of Medicine, New Haven, Connecticut, USA.

[3]Department of Comparative Medicine. Yale University School of Medicine, New Haven, Connecticut, USA.

[4]Genomics and Diabetes Unit, Health Research Institute Clinic Hospital of Valencia (INCLIVA), Valencia, Spain.

[5]Center for Human Nutrition. University of Texas Southwestern Medical Center, Dallas, TX, USA.

[6]Department of Pharmacology Yale University School of Medicine, New Haven, Connecticut, USA

[7]Servicio Bioquímica-Investigación, Hospital Universitario Ramón y Cajal, IRyCIS, Madrid, and CIBER de Fisiopatología de la Obesidad y Nutrición, Instituto de Salud Carlos III, Spain.

[8]Department of Medicine, Cardiology, NYU Grossman School of Medicine, New York, New York, USA

[9]Department of Pathology, NYU Grossman School of Medicine, New York, New York, USA

[10]Department of Microbiology, New York University School of Medicine, New York, NY 10016, USA.

[11]Department of Surgery, Yale University School of Medicine, New Haven, Connecticut, 06520 USA.

Address for Correspondence: Yajaira Suárez, PhD., 10 Amistad Street, Room 320, New Haven, CT 06520. Tel: 203.737.8858. Fax: 203.737.2290. yajaira.suarez@yale.edu, Carlos Fernández-Hernando, PhD., 10 Amistad Street, Room 337c, New Haven, CT 06520. Tel: 203.737.4615. Fax: 203.737.2290. carlos.fernandez@yale.edu.

Disclosures

None

Supplemental Materials

Expanded Methods

Online-only Supplemental Figures S1–8

Online-only Supplemental Figure legends for Figures S1–8

Author Manuscript Author Manuscript Author Manuscript Author Manuscript

[12]Department of Pathology. Yale University School of Medicine, New Haven, Connecticut, USA.

Abstract

Background: Crosstalk between sterol metabolism and inflammatory pathways has been demonstrated to significantly impact the development of atherosclerosis. Cholesterol biosynthetic intermediates and derivatives are increasingly recognized as key immune regulators of macrophages in response to innate immune activation and lipid overloading. 25-hydroxycholesterol (25-HC) is produced as an oxidation product of cholesterol by the enzyme cholesterol 25-hydroxylase (CH25H) and belongs to a family of bioactive cholesterol derivatives produced by cells in response to fluctuating cholesterol levels and immune activation. Despite the major role of 25-HC as a mediator of innate and adaptive immune responses, its contribution during the progression of atherosclerosis remains unclear.

Methods: The levels of 25-HC were analyzed by liquid chromatography-mass spectrometry, and the expression of *CH25H* in different macrophage populations of human or mouse atherosclerotic plaques, respectively. The effect of CH25H on atherosclerosis progression was analyzed by bone marrow (BM) adoptive transfer of cells from WT or *Ch25h*$^{-/-}$ mice to lethally irradiated *Ldlr*$^{-/-}$ mice, followed by a Western diet (WD) feeding for 12 weeks. Lipidomic, transcriptomic analysis and effects on macrophage function and signaling were analyzed *in vitro* from lipid-loaded macrophage isolated from *Ldlr*$^{-/-}$ or *Ch25h*$^{-/-}$;*Ldlr*$^{-/-}$ mice. The contribution of secreted 25-HC to fibrous cap formation was analyzed using a smooth muscle cell (SMC) lineage tracing mouse model, *Myh11*^{ERT2CRE}*mT/mG;Ldlr* $^{-/-}$, adoptively transferred with WT or *Ch25h*$^{-/-}$ mice BM followed by 12 weeks of WD feeding.

Results: We found that 25-HC accumulated in human coronary atherosclerotic lesions and that macrophage-derived 25-HC accelerated atherosclerosis progression promoting plaque instability via autocrine and paracrine actions. 25-HC amplified the inflammatory response of lipid-loaded macrophages and inhibited the migration of SMCs within the plaque. 25-HC intensified inflammatory responses of lipid-laden macrophages by modifying the pool of accessible cholesterol in the plasma membrane, which altered Toll-like receptor 4 (TLR4) signaling, promoted nuclear factor-κB (NFκB)-mediated pro-inflammatory gene expression, and increased apoptosis susceptibility. Interestingly, these effects were independent of 25-HC-mediated modulation of liver X receptor (LXR) or sterol regulatory-element binding protein (SREBP) transcriptional activity.

Conclusions: Production of 25-HC by activated macrophages amplifies their inflammatory phenotype, thus promoting atherogenesis.

Keywords

Atherosclerosis; macrophages; inflammation; 25-hydroxycholesterol

INTRODUCTION

Atherosclerosis is a metabolic and inflammatory disease, characterized by the accumulation of cholesterol-rich lipoproteins and inflammatory cells in the artery wall. Retention of native low-density lipoproteins (LDL) in the intima, favors the formation of oxidized

Author Manuscript Author Manuscript Author Manuscript Author Manuscript

LDLs (Ox-LDL) and other modified lipoproteins, rich in bioactive lipids, that trigger inflammation, leading to subendothelial leukocyte recruitment[1–3]. Recruited monocytes differentiate into macrophages that proliferate[4] and acquire an inflammatory phenotype[5,6]. The inflammatory mediators released by macrophages further activate vascular endothelium, to further promote monocyte recruitment, thus perpetuating a chronic inflammatory state within the artery[7]. Once within the vessel wall, macrophages start scavenging Ox-LDL via surface scavenger receptors[8,9]. Accumulation of cholesterol and other LDL-derived lipids gives rise to lipid-loaded macrophages or foam cells if they are completely filled with lipid droplets[10]. Lipid accumulation may have a beneficial impact[11]; however, in later stages foamy macrophages can be more susceptible to death, promoting a proinflammatory microenvironment. In advanced atherosclerosis, certain lesions evolve into a vulnerable/unstable plaque characterized by necrotic areas rich in dying foam cells, low collagen content, a thin fibrous cap, and non-resolving inflammation[12] that can lead to plaque disruption and acute thrombotic events.

Intracellular cholesterol content is tightly regulated by feedback mechanisms that involve two families of transcription factors, the sterol regulatory element binding proteins (SREBPs) and the liver X receptors (LXRs)[13,14]. SREBP2 drives the transcription of genes involved in cholesterol synthesis and uptake, e.g., hydroxy methyl glutaryl-coenzyme A (*HMG-CoA*) reductase *(HMGCR)* and LDL receptor *(LDLR*), while LXR upregulates cholesterol efflux genes, including ATP-binding cassette A1 *(ABCA1)*[13,14]. Besides controlling cholesterol homeostasis, SREBPs and LXRs regulate inflammation to establish crosstalk with cholesterol metabolism[15–21]. In addition to cholesterol, other sterol intermediates of cholesterol biosynthesis[22] and cholesterol derivatives (oxysterols), such as 25-hydroxycholesterol (25-HC)[23,24] accumulate within the plaque. 25-HC is an oxidation product of cholesterol generated by 25-hydroxylase (CH25H)[25], and reduces cholesterol biosynthesis[25] via inactivation of SREBP2[26,27], stimulates cholesterol efflux through agonism of LXR[13,28–30], and enhances cholesterol esterification by activating Acyl-CoA:cholesterol acyltransferase[31]. However, mice deficient in *Ch25h* have intact cholesterol metabolism[32], challenging the physiological role of 25-HC as a regulator of cholesterol homeostasis[33–35]. On the other hand, *Ch25h* expression is transcriptionally-induced, in macrophages, in response to various inflammatory mediators[32,35–38], thus increasing 25-HC synthesis and participating in immune-related functions. *Ch25h* is an interferon (IFN)-stimulated gene that shows antiviral activities against a range of enveloped viruses[37–39]. These antiviral effects have been linked to the ability of 25-HC to inhibit SREBP2[37,38], to activate LXRs[40], and to reduce cholesterol biosynthesis[37,38]. Other investigations have determined that 25-HC regulates immunoglobulin A production[32], augments the production of some inflammatory cytokines[41,42], and mediates feedback inhibition of interleukin-1 (IL-1) family cytokine production[43] by mediating a type I IFN inhibitory effect on inflammasome activation through repression of SREBP2 activation and concomitant decrease of the cholesterol biosynthetic pathway[44].

Although numerous studies have highlighted the role of 25-HC as a mediator of inflammation-metabolism crosstalk in macrophages, the role of 25-HC in atherosclerosis remains unclear[45,46]. While one study showed that decreased 25-HC via ATF3-mediated repression of *Ch25h* expression, protected against foam cell formation and atherosclerosis[46],

Author Manuscript Author Manuscript Author Manuscript Author Manuscript

another concluded that global *Ch25h* deficiency accelerated atherosclerosis[45]. Here we report that 25-HC accumulates in human coronary atherosclerotic lesions and that *CH25H* is expressed in pro-inflammatory macrophages that populate the plaque. We further show that hematopoietic deficiency of *Ch25h* attenuates the progression of atherosclerosis and promotes lesion stability characterized by reduced plaque necrosis and thicker fibrous cap. Notably, RNA-sequencing (RNA-seq) analysis of lipid-loaded elicited macrophages revealed that *Ch25h* levels, and hence 25-HC, amplifies the inflammatory response of macrophages, increasing the expression of pro-inflammatory genes independently of SREBP2 or LXR-mediated gene transcription. Instead, our findings indicate that these effects were mediated by changes in the pool of accessible cholesterol in the plasma membrane (PM). Furthermore, our data demonstrate that 25-HC did not restrain cholesterol biosynthesis in activated lipid-laden macrophages and did not alter inflammasome activation. Additionally, we demonstrate that activated lipid-laden macrophages release 25-HC into the extracellular media mediating a paracrine effect on SMCs, reducing their migratory phenotype. Altogether, our findings indicate that *CH25H*-mediated production of 25-HC by activated macrophages amplifies their inflammatory phenotype, thus promoting atherogenesis.

METHODS

Detailed methods are provided in the Supplemental Material. The authors declare that all supporting data are available within the article [and its online supplementary files]. Bulk RNA-seq data are accessible in NCBI Gene Expression Omnibus and through GEO Series accession number GSE189079. Data sets from previously published work analyzed in the present study are described in the Supplemental Methods. All animal studies have been approved by the Institutional Animal Care Use Committee of Yale University School of Medicine and conducted in accordance with the National Institutes of Health Guide for the Care and Use of Laboratory Animals. Human samples used in this study are fully described in Supplemental Methods. Briefly, human left main coronary arteries were obtained from the explanted hearts of transplant recipients or cadaver organ donors as described previously[47], and approved by the Institutional Review Boards of Yale University and the New England Organ Bank and were used for liquid chromatography–mass spectrometry (LC/MS-MS) and immunohistochemistry analysis.

Statistical analysis

The number of animals used in each study is listed in the figure legends. *In vitro* experiments were routinely repeated at least three times unless otherwise noted. Analysts were blinded to experimental groups. Data are expressed as average ± SD or ± SEM. Statistical differences were measured using an unpaired two-sided Student's *t*-test, one-way ANOVA and two-way ANOVA with Bonferroni correction for multiple comparisons. Normality was checked using the Kolmogorov-Smirnov test. A nonparametric test (Mann-Whitney) was used when data did not pass the normality test or sample size was small. A value of $P \leq 0.05$ was considered statistically significant. Data analysis was performed using GraphPad Prism Software Version 7 (GraphPad, San Diego, CA). For Bulk RNA-seq, the Differential Gene Expression-GSA algorithm was implemented. A default P-value < 0.05

Author Manuscript Author Manuscript Author Manuscript Author Manuscript

was considered statistically significant with a fold-change > 1.5 for up-regulated transcripts or < −1.5 for down-regulated transcripts.

RESULTS

Human and mouse pro-inflammatory atherosclerotic plaque macrophages exhibit increased *CH25H* mRNA levels

We have previously described that 25-HC is present in atherosclerotic mouse aortas[24]. To understand the relevance of 25-HC in atherosclerosis, we analyzed the levels of 25-HC in human coronary arteries with mild, moderate, and severe atherosclerotic plaques (Figure 1A) by LC/MS-MS (Figure 1B). We found that plaques with more severe atherosclerosis presented higher levels of 25-HC (Figure 1B). Interestingly, this finding is in line with higher macrophage content ($CD68^+$ cells) in these plaques (Figure 1A), suggesting that 25-HC levels are related to the accumulation of macrophages within the plaque.

Next, we analyzed the expression of *CH25H* in macrophages from human[48] (Figure 1C) and mouse (Figure 1D and Figures S1) atherosclerotic plaques[10,49]. Single cell RNA-seq (scRNA-seq) revealed that macrophages from human atherosclerotic plaques with a pro-inflammatory gene signature exhibited more cells with high *CH25H* mRNA levels (Figure 1C). ScRNA-seq analysis from total leukocytes obtained from $Ldlr^{-/-}$ aortas[10] showed that inflammatory clusters of aortic macrophages, Clusters B ($Trem2^{lo}$, Tnf^+) and C ($Trem2^{lo}$, $Gbp4^+$,$Mx1^+$), exhibited more cells with high levels of *Ch25h*, whereas in non-inflammatory clusters, Clusters A ($Trem2^{hi}$, $Fabp5^+$) or D ($Trem2^{lo}$, $Mrc1^+$, $Lyve1^+$) exhibited fewer cells expressing high levels of *Ch25h* (Figure 1D and Figure S1A–C). Similar results were obtained by analyzing a different scRNA-seq data set from cells obtained from $Ldlr^{-/-}$ aortas[49] with equivalent macrophage clusters (Figure S1G–J). Furthermore, bulk RNA-seq analysis of intimal macrophages isolated from *Apolipoprotein E* (*Apoe*) deficient murine aortas[10] (Figure S1D), manifested that foamy ($BODIPY^{hi}$, Side Scatter/SSC^{hi}) non-inflammatory macrophages exhibited diminished *Ch25h* expression when compared to inflammatory macrophages with a broad range of lipid-loading but with no evident signs of lipid droplet accumulation ($BODIPY^{lo}$,SSC^{lo}).

Collectively, these results indicate that 25-HC accumulates in the artery wall during atherogenesis and that *CH25H* is expressed at higher levels in both human and mouse pro-inflammatory plaque macrophages, suggesting that 25-HC is associated with inflammation and atherosclerosis.

Hematopoietic *Ch25h* deficiency diminishes the progression of atherosclerosis

To determine the *in vivo* function of *Ch25h* and, hence 25-HC, during the progression of atherosclerosis, we transplanted bone marrow (BM) cells from WT or $Ch25h^{-/-}$ mice to lethally irradiated $Ldlr^{-/-}$ mice (hence forth referred to as WT→$Ldlr^{-/-}$ and $Ch25h^{-/-}$→$Ldlr^{-/-}$ mice), followed by a WD feeding for 12 weeks. We determined the levels of 25-HC in lipid extracts from $Ch25h^{-/-}$→$Ldlr^{-/-}$ mouse aortas (Figure S2A). 25-HC was undetectable, whereas other oxysterols (e.g., 27-HC or 24-HC) and sterols such as desmosterol were detectable. Interestingly, 27-HC, an oxysterol produced from cholesterol

Author Manuscript Author Manuscript Author Manuscript Author Manuscript

by cytochrome P450 family 27 subfamily A (Cyp27a), which is almost specifically expressed in macrophages (Figure S1E and F, see also S1B and H), was efficiently detected in the aortas of *Ch25h*$^{-/-}$→*Ldlr*$^{-/-}$ mice (Figure S2A). Thus, in atherosclerotic murine aortas, 25-HC is mostly produced by hematopoietic cells and the contribution of other cell types from the recipient *Ldlr*$^{-/-}$ mice to the production of 25-HC is negligible. These results are in line with almost exclusive expression of *Ch25h* in macrophages when compared to other cell types present in mouse aortas (Figure S1F).

Histological analysis of the aortic root revealed that *Ch25h*$^{-/-}$→*Ldlr*$^{-/-}$ mice developed smaller lesions than WT→*Ldlr*$^{-/-}$ mice (Figure 2A). Although oil red O (ORO) staining in the aortic root did not show differences in the accumulation of neutral lipids (Figure S2B), *en face* analysis of the whole aorta showed reduced lipid accumulation in *Ch25h*$^{-/-}$→*Ldlr*$^{-/-}$ mice (Figure 2B). Additional morphological analysis of the aortic roots revealed that *Ch25h*$^{-/-}$→*Ldlr*$^{-/-}$ mice had smaller necrotic cores (Figure 2C) and increased collagen content (Figure 2D), indicating more stable atherosclerotic lesions. All these effects were observed with no statistical differences in body weight, plasma lipid levels, or circulating leukocytes (Figure S3A–H).

Complex advanced lesions are characterized by the accumulation of macrophages, SMCs, and dead cells that in turn promote chronic inflammation within the artery wall[12]. Immunodetection in the aortic root for CD68 positive macrophages or smooth alpha actin (SMA) positive SMCs showed that *Ch25h*$^{-/-}$→*Ldlr*$^{-/-}$ mice exhibited reduced CD68-positive plaque area and increased SMA-positive area when compared to WT→*Ldlr*$^{-/-}$ mice (Figure 3A). The decrease in macrophage content within the plaques of *Ch25h*$^{-/-}$→*Ldlr*$^{-/-}$ mice was accompanied by reduced inflammation, as indicated by reduced plasma levels of circulating pro-inflammatory mediators, including chemokine (C-X-X) motif ligand 1 (CXCL1), 9 (CXCL9) and the monocyte chemoattractant protein-1 (MCP-1) or CCL2 (Figure S2C), as well as reduced immunodetection of vascular cell adhesion molecule-1 (VCAM-1) (Figure 3B). In agreement with the reduced necrotic core area (Figure 2B), we found that *Ch25h*$^{-/-}$→*Ldlr*$^{-/-}$ mice had reduced numbers of TUNEL-positive CD68-positive cells within plaques than control mice (Figure 3C). These findings indicated that loss of *Ch25h* in hematopoietic cells reduced the progression of atherosclerosis and promoted plaque stability by decreasing vascular inflammation and reducing macrophage accumulation and death within the lesions.

25-HC promotes the expression of inflammatory genes in lipid-laden macrophages

To elucidate the contribution of *Ch25h* in regulating atherogenic phenotypes, we isolated thioglycolate-elicited peritoneal macrophages (TG-EPM) from hypercholesterolemic mice, which accumulate and store broad amounts of lipids in the cytosol, mimicking the lipid-loaded macrophages present in atherosclerotic lesions[50–52], and profiled their transcriptomes by RNA-seq (Figure S4 and Figures 4 and 5). Macrophages from both *Ldlr*$^{-/-}$ or *Ch25h*$^{-/-}$;*Ldlr*$^{-/-}$ mice exhibited increased neutral lipid accumulation when compared to mice (WT or *Ch25h*$^{-/-}$) that were not on the *Ldlr*$^{-/-}$ background (Figure S5A). However, the absence of *Ch25h* did not affect the accumulation of neutral lipids (Figure S5B). TG-EPM from *Ldlr*$^{-/-}$ or *Ch25h*$^{-/-}$;*Ldlr*$^{-/-}$ mice were stimulated for 4 or 12 h with lipopolysaccharide

Author Manuscript Author Manuscript Author Manuscript Author Manuscript

(LPS) to increase basal expression levels of *Ch25h*[36,37,38,41,53,54]. As expected, LPS stimulation of control *Ldlr*$^{-/-}$ macrophages increased *Ch25h* mRNA levels (Figure 4A), which was accompanied with an increase in intracellular 25-HC[36] (Figure 4B). This effect was not observed in *Ch25h*$^{-/-}$;*Ldlr*$^{-/-}$ elicited macrophages (Figure 4A and B). In mock-treatment conditions, ~ 200 genes were differentially and significantly expressed (FC>1.5, $P \leq 0.05$) in *Ch25h*$^{-/-}$;*Ldlr*$^{-/-}$ macrophages when compared to control *Ldlr*$^{-/-}$ (Figure 4C). Kyoto Encyclopedia of Genes and Genomes (KEGG) pathway enrichment analysis showed that extracellular matrix remodeling factors were over-represented in *Ch25h*$^{-/-}$;*Ldlr*$^{-/-}$ macrophages (Figure 4D, *upper panel*). However, after 4 h of LPS stimulation there were more than 500 differentially expressed genes in *Ch25h*$^{-/-}$;*Ldlr*$^{-/-}$ *vs. Ldlr*$^{-/-}$ macrophages (Figure 4C). The vast majority of these genes were downregulated, and KEGG pathway enrichment analysis revealed that pathways related to macrophage inflammatory response were over-represented in *Ch25h*$^{-/-}$;*Ldlr*$^{-/-}$ mice (Figure 4D, *lower-left panel*). Interestingly, transcripts of the TLR4-induced transcriptional program, including NFκB, activator protein-1 (AP-1), and interferon regulatory factors (IRFs) (e.g., *Rela, Nfkb2, Irf5, Jund*), as well as genes that encode cytokines and chemokines (e.g., *Tnf, Cxcl10, Il12a, Ccl5*) were significantly downregulated in *Ch25h*$^{-/-}$;*Ldlr*$^{-/-}$ macrophages (Figure 4E). Remarkably, within the upregulated transcripts in *Ch25h*$^{-/-}$;*Ldlr*$^{-/-}$ macrophages, we found numerous anti-inflammatory genes (e.g., *Il10, Arg1, Mrc1*) (Figure 4E). After 12 h of LPS stimulation, *Ch25h*$^{-/-}$;*Ldlr*$^{-/-}$ macrophages presented 552 differentially regulated transcripts. In this case, most of the genes were up-regulated (Figure 4C) and pathways related to macrophage phagocytic activity were over-represented (Figure 4D, *lower-right panel*). Specifically, genes involved in phagocytosis (e.g., *Mrc1, Cd36, Fcgr1, Cyba*), lysosomal activity (e.g., *Ctsl, Atp6v0b, Lgmn, Psap*) and intracellular cholesterol transport (e.g., *Npc2, Stard3*, *Tspo)* were significantly upregulated (Figure 4F). Interestingly, the genes that were downregulated in *Ch25h*$^{-/-}$;*Ldlr*$^{-/-}$ macrophages were also pro-inflammatory (e.g., *Il6, Il12b, Cxcl9*) (Figure 4F).

To identify molecules that potentially participate in the observed changes in gene expression, we used Ingenuity Pathway Analysis (IPA®) to identify potential upstream regulators and focused the analysis on transcription factors (TFs). Upstream regulator analysis after 4 h of LPS stimulation predicted inactivation of the pro-inflammatory TFs NFκB, STAT1 and IRF3 in *Ch25h*$^{-/-}$;*Ldlr*$^{-/-}$ *vs. Ldlr*$^{-/-}$ macrophages (Figure 4G). This aligns with the decreased levels of *Tnf, Cxcl10, Il12a*, and *Ccl5* in *Ch25h*$^{-/-}$;*Ldlr*$^{-/-}$ macrophages (Figure 4E). On the other hand, the anti-inflammatory TF STAT6 was predicted to be activated (Figure 4G), in line with increased levels of some of its targets genes, such as *Arg1* and *Mrc1*[55], in *Ch25h*$^{-/-}$;*Ldlr*$^{-/-}$ macrophages (Figure 4E). After 12 h of TLR4 stimulation, upstream analysis predicted that the TFs STAT3, NFE2L2, and SMAD3 were activated in *Ch25h*$^{-/-}$;*Ldlr*$^{-/-}$ macrophages (Figure 4H). STAT3 is crucial for the suppressive effect of IL-10 on LPS-induced genes[56]. NFE2L2-NFκB interplay regulates inflammatory responses[57]. NFE2L2 negatively regulates the transcription of *Il6*[58], which is also a pro-inflammatory cytokine gene downregulated in *Ch25h*$^{-/-}$;*Ldlr*$^{-/-}$ macrophages (Figure 4F). SMAD3 has been shown to promote a phagocytic phenotype in macrophages[59]. Activation of SMAD3 could account for the increase in some phagocytic genes, including *Mfge8*, that are observed in *Ch25h*$^{-/-}$;*Ldlr*$^{-/-}$ macrophages (Figure 4F).

Author Manuscript Author Manuscript Author Manuscript Author Manuscript

These results indicate that hypercholesterolemic *Ch25h*$^{-/-}$ macrophages, that do not synthesize 25-HC upon TLR4-stimulation, exhibit a reduced pro-inflammatory gene signature and a pro-resolving transcriptional profile. This suggests that 25-HC synthesis by macrophages during atherosclerosis amplifies inflammation.

25-HC in lipid-laden macrophages does not promote LXR activation or the repression of SREBP2 activation.

SREBP and LXR transcription factor families are well known as master regulators of cholesterol homeostasis and are also implicated in macrophage inflammatory response[13,20,21,29,44]. Previous studies have established that 25-HC acts as a ligand for LXRs[11,13] and as a repressor for SREBPs[23]. However, there is only limited *in vivo* evidence that 25-HC functions via these pathways in the context of lipid-laden macrophages. We analyzed how the levels of LXR[60] and SREBP[61] target genes were altered in our RNA-seq data set. We found that the activation and repression of LXR target genes after TLR4 stimulation was similar regardless of *Ch25h* expression (Figure 5A). *Ch25h*$^{-/-}$*;Ldlr*$^{-/-}$ macrophages exhibited almost the same number of upregulated LXR target genes as control *Ldlr*$^{-/-}$ macrophages after 4 h of LPS stimulation. However, after 12 h of TLR4 stimulation, more LXR target genes were upregulated in *Ch25h* deficient macrophages than in *Ldlr*$^{-/-}$ macrophages (Figure 5B), despite the latter accumulating substantial amounts of 25-HC (Figure 4B), suggesting that 25-HC was not required for LXR activation. Moreover, comparing the normalized counts of well-established LXR target genes (e.g., *Abca1, Abcg1, Lpl, Mylip, Pltp, Plin2*) at different time points after LPS treatment, did not reveal significant differences between the genotypes (Figure S5A).

Next, we analyzed mRNA levels of classical SREBP2 target genes in LPS treated TG-EPM from *Ldlr*$^{-/-}$ or *Ch25h*$^{-/-}$*;Ldlr*$^{-/-}$ mice. We found an overall reduction in the expression of SREBP2 target genes after 4 hours of LPS stimulation in control *Ldlr*$^{-/-}$ macrophages (Figure 5C). However, after 12 hours of LPS stimulation, the expression of SREBP2 target genes were elevated compared to the mock-treated macrophages (Figure 5C). Interestingly, *Ch25h* deficiency did not alter this pattern of expression (Figure 5C); indeed, the mRNA levels of several well-known SREBP2 target genes (e.g., *Hmgcs1, Hmgcr, Hmgcl, Cyp51, Ebp, Scd5, Dhcr7, Dhcr24*) were similar in *Ch25h*$^{-/-}$*;Ldlr*$^{-/-}$ *vs. Ldlr*$^{-/-}$ macrophages (Figure S6B). To further evaluate the contribution of 25-HC to the regulation of cholesterol biosynthesis in lipid-laden macrophages, we employed LC/MS-MS to quantify alterations in sterol intermediates because of 25-HC-mediated regulation of SREBP2 signaling. As described above, control *Ldlr*$^{-/-}$ macrophages but not *Ch25h*$^{-/-}$*;Ldlr*$^{-/-}$ accumulated 25-HC (Figure 4B). However, the absence or presence of 25-HC in macrophages did not alter the amount of key sterol intermediates such as lanosterol, 24,25-dehydrolanosterol, 7-dehydrodesmosterol, 7-dehydrocholesterol or desmosterol. Only increased levels of zymosterol were found in *Ch25h*$^{-/-}$*;Ldlr*$^{-/-}$ macrophages (Figure 5D).

Altogether, our results indicate that in activated lipid-loaded macrophages, 25-HC does not significantly alter SREBP or LXR-mediated gene expression and, that the accumulation of sterol intermediates in cholesterol biosynthesis after inflammatory stimulation is independent of the presence of 25-HC.

Author Manuscript Author Manuscript Author Manuscript Author Manuscript

25-HC in activated lipid-laden macrophages reduces cell survival and efferocytosis capacity

To explore the effect of 25-HC on cell death, we first analyzed how the absence of *Ch25h* affects susceptibility to LPS-induced apoptosis[62]. As shown in Figure 6A, after LPS stimulation, lipid-laden *Ch25h*$^{-/-}$;*Ldlr*$^{-/-}$ macrophages presented reduced active/cleaved caspase 3 levels when compared to *Ldlr*$^{-/-}$ counterparts, in agreement with the reduced TUNEL-positive CD68-positive cells found in plaques from *Ch25h*$^{-/-}$→*Ldlr*$^{-/-}$ mice (Figure 3C). This suggests that a lack of 25-HC synthesis in activated lipid-laden macrophages reduced apoptosis susceptibility. Additionally, we studied caspase-1 activation, as a read-out of inflammasome activation, given that pyroptosis is an inflammasome-dependent form of cell death that occurs within atherosclerotic plaques[63], and that 25-HC regulates inflammasome activation[43,44]. As shown in Figure 6B, *Ch25h*$^{-/-}$;*Ldlr*$^{-/-}$ macrophages exhibited a significant increase in pro-IL-1β protein despite *Il1b* mRNA levels being unchanged. Regardless, we did not find differences in inflammasome activation or IL-1β secretion between *Ldlr*$^{-/-}$ and *Ch25h*$^{-/-}$;*Ldlr*$^{-/-}$ foamy macrophages (Figure 6B). This is in contrast with previous work that has shown that *Ch25h*$^{-/-}$ macrophages exhibit increased inflammasome activation and IL-1β secretion[43,44]. However, in non-lipid-laden BM-derived macrophages, we observed increased levels of active caspase-1 and secreted IL-1β, in line with previous work[43] (Figure S7A).

Since previous studies have correlated 25-HC synthesis to mitochondrial reactive oxygen species (ROS) production[44,64] and because disbalance in mitochondrial ROS can lead to apoptosis, we also measured mitochondrial mass and mitochondrial ROS production by flow cytometry in LPS-stimulated TG-EPM form *Ldlr*$^{-/-}$ and *Ch25h*$^{-/-}$;*Ldlr*$^{-/-}$ mice. As shown in Figure S7 B and C, there were no statistical differences in mitochondrial mass or ROS production. These results suggest that in lipid-laden macrophages, the reduced susceptibility to LPS-induced apoptosis observed in *Ch25h*$^{-/-}$;*Ldlr*$^{-/-}$ macrophages (Figure 6A) could be unrelated to inflammasome activation or mitochondrial ROS production. RNA-seq analysis revealed that activated *Ch25h*$^{-/-}$;*Ldlr*$^{-/-}$ lipid-laden macrophages showed reduced mRNA levels of *Tnf (*Figure 4E), and autocrine secretion of TNF has been involved in LPS-induced apoptosis[62]. Alternatively, activated *Ch25h*$^{-/-}$;*Ldlr*$^{-/-}$ lipid-laden macrophages showed increased levels of *Cd5l* (Figure S7D), which is highly expressed in foamy macrophages within atherosclerotic lesions (Figure S1B,C, H and I) and protective[65–67], promoting their survival[68]. These findings are in line with the diminished inflammatory and apoptotic phenotype exhibited by *Ch25h*$^{-/-}$;*Ldlr*$^{-/-}$ lipid-laden macrophages.

We also found that *Ch25h*$^{-/-}$;*Ldlr*$^{-/-}$ macrophages displayed increased efferocytotic capacity compared to *Ldlr*$^{-/-}$ macrophages (Figure 6C). This correlates with increased mRNA levels of several efferocytosis genes such as *Gas6, C1q, Mfge8* and *Itgb3* found in *Ch25h*$^{-/-}$;*Ldlr*$^{-/-}$ macrophages (Figure 4F). Furthermore, *Mertk* expression was found in macrophage clusters with low or no detectable *Ch25h* expression (Figure S1B and H). To evaluate the biological relevance of this finding, we analyzed *in situ* efferocytosis by counting the number of macrophage-associated apoptotic cells *vs*. free apoptotic cells in individual aortic root sections[69–72]. As shown in Figure 6D, *Ch25h*$^{-/-}$→*Ldlr*$^{-/-}$ mice exhibit a higher ratio of macrophage-associated to free apoptotic cells, consistent with the improved

Author Manuscript Author Manuscript Author Manuscript Author Manuscript

efferocytotic activity observed in the absence of *Ch25h*. These results agree with the smaller necrotic core found in *Ch25h*$^{-/-}$→*Ldlr*$^{-/-}$ mice (Figure 2B) and reveal that in the absence of 25-HC production, lipid-laden activated macrophages have improved efferocytosis and are more resistant to inflammation-induced apoptosis.

Absence of 25-HC alters cell membrane composition, resulting in a reduction in the TLR4/p38/NFkB signaling cascade

As shown above, *Ch25h*$^{-/-}$;*Ldlr*$^{-/-}$ lipid-laden macrophages had reduced expression of inflammatory genes after LPS stimulation when compared to control *Ldlr*$^{-/-}$ macrophages. Interestingly, *Tnf, Il12a* and *Il6* were among the significantly downregulated genes (Figure 4E), that are indeed hallmarks of both NF-κB and AP-1 activation[55]. Thus, we wondered whether TLR4 signaling was affected in *Ch25h*$^{-/-}$;*Ldlr*$^{-/-}$ lipid-laden macrophages to account for the reduced expression of inflammatory genes. LPS/TLR4 signaling can be divided into MyD88-dependent and MyD88-independent pathways, which mediate the activation of pro-inflammatory cytokines and type I IFN induced genes, respectively. Hence, we first analyzed the activation of three key proteins in the MyD88-dependent and independent pathways, p65, MAP-kinase p38, and IRF3. As shown in Figure 7A, after long exposure to LPS, *Ch25h*$^{-/-}$;*Ldlr*$^{-/-}$ macrophages exhibited significantly reduced activation (phosphorylation) of p38 and IRF3 than *Ldlr*$^{-/-}$ macrophages. Similar results were also observed under acute TLR4 stimulation (Figure 7B), in this case with reduced phosphorylation of p65. Interestingly, we also found a delay in the p38 activation peak, from 15 minutes in *Ldlr*$^{-/-}$ macrophages to 30 min in *Ch25h*$^{-/-}$;*Ldlr*$^{-/-}$ macrophages. The IRF3 activation peak went from 30 min in *Ldlr*$^{-/-}$ macrophages to 60 min in *Ch25h*$^{-/-}$;*Ldlr*$^{-/-}$ macrophages (Figure 7B). Altogether, these results indicate that absence of 25-HC in *Ch25h*$^{-/-}$;*Ldlr*$^{-/-}$ macrophages downregulates both TLR4 signaling branches. Since the accumulation of free cholesterol in the PM can hypersensitize macrophages to LPS[73–77], we used the fluorescently-labeled, non-lytic cholesterol-binding protein, Anthrolysin O domain 4 (ALOD4), to measure the amount of accessible cholesterol in the PM of *Ch25h*$^{-/-}$;*Ldlr*$^{-/-}$ and *Ldlr*$^{-/-}$ lipid-laden macrophages by flow cytometry. As shown in Figure 7C, we found a diminished accumulation of accessible cholesterol in the PM of *Ch25h*$^{-/-}$;*Ldlr*$^{-/-}$ macrophages in comparison to control *Ldlr*$^{-/-}$. Although mRNA levels of membrane cholesterol transporters *Abca1* and *Abcg1* were similar in the presence or absence of *Ch25h* (Figure S5), *Ch25h*$^{-/-}$;*Ldlr*$^{-/-}$ macrophages showed higher protein levels of both ABCA1 and ABCG1 (Figure S7E). Of interest, *Abca1*- and *Abcg1*-deficient peritoneal macrophages have enhanced inflammatory responses which is associated with increased membrane free cholesterol[76]. These results suggests that the reduction in TLR4-mediated signaling that we observed in hypercholesterolemic *Ch25h*$^{-/-}$;*Ldlr*$^{-/-}$ macrophages could be due to diminished free cholesterol in the PM. Thus, we pre-treated the cells with sphingomyelinase (SMase), to release cholesterol sequestered by sphingomyelin to increase the pool of accessible cholesterol in the PM[78,79], prior to the stimulation with LPS and assessed p65 activation. Cells were also incubated with anthrolysin O peptide (ALOD4) to concomitantly measure accessible free cholesterol. SMase pre-treatment increased ALOD4 binding in both groups of macrophages (Figure 7D). Interestingly, the SMase-mediated increase of free cholesterol in the PM of *Ch25h*$^{-/-}$;*Ldlr*$^{-/-}$ macrophages rescued the reduced activation of p65 observed in *Ch25h*$^{-/-}$;*Ldlr*$^{-/-}$ in the absence of SMAse (Figure 7B),

Author Manuscript Author Manuscript Author Manuscript Author Manuscript

resulting in comparable levels of p65 activation to that present in *Ldlr*$^{-/-}$ macrophages in the absence of SMase (Figure 7D). These results indicate that in activated lipid-laden macrophages, lack of 25-HC production decreases TLR4-mediated signaling, at least in part by altering the accumulation of free cholesterol in the PM.

25-HC is released by activated macrophages to inhibit SMC migration

Activated macrophages release 25-HC into the extracellular space with a paracrine effect on cells in the immediate vicinity[32,38,41]. In consonance, we found that LPS-stimulated lipid-laden macrophages release 25-HC to the media in a time-dependent manner, while macrophages deficient in *Ch25h* did not (Figure 8A). In both cases, the secretion of other oxysterols (e.g., 24-HC or 27-HC) was unaltered (Figure 8A). Since migration of SMCs from the tunica media into the intima is a key event for fibrous cap formation, collagen deposition, and plaque stability, and we found an increase in SMC content within the plaques of *Ch25h*$^{-/-}$→*Ldlr*$^{-/-}$ mice, we sought to investigate whether 25-HC influences cellular responses of SMCs during atherogenesis. We analyzed the effect of 25-HC on SMC migration in response to platelet-derived growth factor (PDGF) in a trans-well assay. As shown in Figure 8B pretreatment of VSMCs with 25-HC reduced PDGF-induced migration. These findings suggest that macrophage-derived 25-HC reduces SMC migration to populate the fibrous cap. Since PDGF receptor β (PDGFRβ) is relocated into cholesterol-rich domains within the PM for proper intracellular signaling transduction[80] and the pool of free cholesterol in the PM is altered when cells are treated with 25-HC[23], we investigated whether 25-HC alters PDGFRβ signaling in SMC. As expected, addition of 25-HC into the culture media reduced the amount of free cholesterol in the PM of SMC (Figure 8C) without affecting cell viability, since total cell number was not affected (Figure S8A). In line with this, SMC pretreated with 25-HC showed decreased phosphorylated protein kinase B (*aka* AKT) and extracellular signal-regulated kinase (ERK1/2) after stimulation with PDGF, suggesting that 25-HC diminishes PDGFRβ signaling, in part by altering the pool of free cholesterol in the PM. Furthermore, dorsal ruffle formation after PDGF stimulation[81], an early event in cell migration, was reduced when SMC were pretreated with 25-HC (Figure S8B) These findings suggest that macrophage-derived 25-HC may alter PDGF signaling in SMC and thus affecting their migration.

To validate these *in vitro* results and to understand the contribution of macrophage-derived 25-HC to fibrous cap formation, we used a SMC lineage tracing mouse model (*Myh11*^{ERT2CRE}*mT/mG;Ldlr*$^{-/-}$) since SMCs within the atherosclerotic plaque cannot solely be identified by SMA staining[82], and performed BM adoptive transfer using WT or *Ch25h*$^{-/-}$ mice as BM donors to study the progression of atherosclerosis. After 12 weeks on WD, reporter mice that received *Ch25h*$^{-/-}$ BM showed a significant increase in enhanced green fluorescence protein (eGFP)$^{+}$ SMCs within the plaque (Figure 8E) primarily due to accumulation within the fibrous cap (Figure 8E). These findings suggest that expression of *Ch25h*, and consequent production of 25-HC by macrophages reduces the migration of SMCs that populate the fibrous cap, thus promoting plaque instability.

Author Manuscript Author Manuscript Author Manuscript Author Manuscript

DISCUSSION

In this study we determined that macrophage-derived 25-HC accelerates atherosclerosis progression and promotes plaque instability. We found that, in lipid-laden macrophages, lack of 25-HC production favors lower levels of accessible cholesterol in the PM, which alters TLR4 signaling, decreases NFκB-mediated pro-inflammatory gene expression, and reduces apoptosis susceptibility. These effects are not a result of 25-HC-mediated modulation of LXR or SREBP transcription. Interestingly, unlike other oxysterols, 25-HC is released by activated macrophages as a secondary messenger that inhibits SMC migration, contributing to plaque instability.

Our *in vivo* studies demonstrate that hematopoietic *Ch25h* deficiency significantly reduces atherosclerosis and enhances plaque stability. Our results align with a previous study that showed that ATF3-mediated suppression of *Ch25h* reduces atherosclerosis[46], while another study by Li *et al.* showed that *Ch25h* deficiency promoted atherosclerosis[45]. The discrepancies could be due to the differences in the animal model approach used. While we used a BM adoptive transfer approach in $Ldlr^{-/-}$ mice to determine the role of *Ch25h* in hematopoietic cells, and hence macrophages, Li *et al.* used a global *Ch25h* knockout in the atherogenic $Apoe^{-/-}$ background. With this approach, the effect of *Ch25h* deficiency in other tissues (e.g., liver and adipose tissue) and its participation in atherosclerotic progression could not be ruled out. On the other hand, in a model of diet-induced obesity, global deficiency of *Ch25h* reduces adipose tissue inflammation[83]. Additionally, it has been shown that $Ch25h^{-/-}$ mice are protected against inflammatory-induced pathology in a model of influenza infection[41]. These results, together with the findings of our present study, support the idea that 25-HC promotes inflammation *in vivo*.

To understand the molecular mechanisms that underlie the proatherogenic effects of macrophage-derived 25-HC, we performed RNA-seq in lipid-laden macrophages. We stimulated macrophages with LPS for 4 or 12 h to mimic an activation phase and resolution phase of inflammation[19]. In the activation phase, *Ch25h* deficiency reduced the expression of inflammatory genes, which agrees with previous studies showing that BM derived macrophages (BMDMs) isolated from $Ch25h^{-/-}$ mice have reduced levels of *Nos2, Il12b, Il6* and *Tnf* after LPS-mediated TLR4 stimulation[41,83]. In line with this, we also found that aortic macrophages from atherosclerotic mice with reduced expression of inflammatory genes also had reduced *Ch25h* levels. Mechanistically, we found that the absence of 25-HC synthesis decreased the accumulation of accessible cholesterol in the PM and increased ABCA1 and ABCG1 protein levels, altogether resulting in reduced TLR4 mediated signaling and diminished NFκB-mediated transcription of inflammatory genes. This aligns with previous studies that have demonstrated that macrophages deficient in cholesterol *Abc* transporters accumulate free cholesterol in the PM, increasing TLR4-dependent signaling[73,74, 75–77]. Interestingly, the accumulation of sterols is quite different. While $Abcg1^{-/-}$ macrophages accumulate 7-ketocholesterol and desmosterol, as well as 27-OH, the absence of *Ch25h* promotes the accumulation of zymosterol. This indicates that the underlying effect on inflammation could not be attributed to a specific sterol and that all may contribute to the observed effect in PM cholesterol composition, or that other factors could be responsible for the phenotype. Indeed, diminished p38 activation upon the absence of

Author Manuscript Author Manuscript Author Manuscript Author Manuscript

25-HC synthesis in *Ch25h*$^{-/-}$;*Ldlr*$^{-/-}$ macrophages could influence ABCG1 phosphorylation and degradation[84] and, therefore increase ABCG1 protein levels. Altogether, our results indicate that deficiency in 25-HC production alters free cholesterol PM composition and macrophage responses to inflammatory stimulus.

In the resolution phase, lipid-laden *Ch25h* deficient macrophages were transcriptionally reprogrammed into a pro-phagocytic phenotype, which was supported by the in *vitro* and *in situ* efferocytosis assays. This is in contrast with recent work showing that 25-HC production promotes efferocytosis in alveolar and peritoneal macrophages[85]. However, in our efferocytosis experiments, macrophages were stimulated with LPS before co-culture with apoptotic cells to increase the expression of *Ch25h* and hence the amount of 25-HC in *Ldlr*$^{-/-}$ control macrophages. In the presence of LPS, the efferocytosis mediator MERTK is cleaved from the macrophage membrane surface by the metalloprotease ADAM17 in a p38-dependent manner, thus reducing macrophage efferocytosis capacity[86]. Since in the absence of *Ch25h*, TLR4 stimulated signaling and p38 activation are reduced, it is possible that *Ch25h*$^{-/-}$;*Ldlr*$^{-/-}$ macrophages conserve more MERTK on the surface after LPS treatment, which could explain their increased efferocytotic activity. This is in line with the increased expression of *Mertk* in aortic macrophage clusters with low or nondetectable levels of *Ch25h*. Nevertheless, our *in vivo* data showed that absence of hematopoietic *Ch25h* reduces necrotic core area and the accumulation of dead macrophages in the plaque, due to more efficient efferocytosis. A second factor that influences necrosis in atherosclerotic plaques is extensive apoptosis that occurs in lesions[87]. In this regard, *Ch25h*$^{-/-}$;*Ldlr*$^{-/-}$ macrophages have increased levels of the pro-survival gene *Cd5l*, which has been reported to protect lipid-laden macrophages from apoptosis[68], and make them less susceptible to LPS-induced apoptosis[65–67]. Furthermore, *Cd5l* expression was restricted to foamy and non-inflammatory macrophage clusters with barely detectable levels of *Ch25h* expression. These results demonstrate that 25-HC increases cell apoptosis, reduces efferocytosis and promotes inflammation, three hallmarks of defective inflammatory resolution.

For many years, 25-HC has been proposed to regulate cholesterol metabolism[26], and it has been demonstrated that 25-HC added into culture media suppresses SREBP proteolytic processing[88, 26,89] and activates LXR-mediated gene expression[30,89]. On the other hand, animals deficient in *Ch25h* do not exhibit any alteration in cholesterol metabolism[32] and there is no evidence that *Ch25h* knockout animals have altered SREBP or LXR transcriptional activity. However, a recent study showed that 2h after LPS inhalation, WT animals had increased 25-HC in the lungs, and several LXR target genes (e.g., *Abca1, Abcg1, Srebf1, Nr1h3* and *Nr1h2*) were upregulated, while this response was not present in *Ch25h* deficient mice[85]. Our data obtained in TG-EPM from hypercholesterolemic *Ch25h*$^{-/-}$;*Ldlr*$^{-/-}$ mice indicate unaltered LXR transcriptional activity in basal and stimulated conditions, i.e., no significant differences in mRNA levels of more than 300 validated LXR target genes[60] when compared to *Ldlr*$^{-/-}$ macrophages. However, it is possible that the effect described by Madenspatcher *et al.* in some specific LXR target genes[85] can be buffered in our model, since LXR activity is presumably higher in lipid-loaded macrophages. In line with this, accumulation of desmosterol, an endogenous LXR ligand[24,50], was not altered in the absence or presence of 25-HC. Similarly, secreted levels of the LXR ligand, 27-HC, that normally correlate with its cellular

Author Manuscript Author Manuscript Author Manuscript Author Manuscript

levels, were unaltered in *Ldlr*$^{-/-}$ and *Ch25h*$^{-/-}$;*Ldlr*$^{-/-}$ macrophages. Furthermore, while TLR4-stimulated normolipidemic BMDMs downregulate *Cyp51* expression and accumulate lanosterol to diminish innate immune responses[36], lipid-laden peritoneal macrophages did not exhibit this effect regardless of the absence or presence of 25-HC. This also provides relevance of our results to hypercholesterolemic proatherogenic conditions.

In normolipidemia, increased 25-HC production after pathogen recognition reduces SREBP2 activity and cholesterol biosynthesis to prevent cholesterol-dependent mitochondrial dysfunction and inflammasome activation[43,44]. In lipid-laden macrophages, we did not find any alteration in mitochondrial ROS production or inflammasome activation in *Ch25h*$^{-/-}$;*Ldlr*$^{-/-}$ macrophages compared to *Ldlr*$^{-/-}$ controls. This is consistent with unchanged mRNA levels of SREBP2 target genes, cholesterol, or desmosterol levels, which have also been associated with mito-ROS production and NLRP3-dependent inflammasome activation[24], further indicating that 25-HC does not restrain SREBP2 activation and cholesterol biosynthesis in this setting. On the other hand, they suggested that *Ch25h* is not necessary for the initial downregulation of cholesterol biosynthesis but required to maintain this effect over time in a mTORC1-dependent manner[44]. Lysosomes are key for mTORC1 signaling[90] and disturbances in lysosome biology have a clear impact on mTORC1 activation[90]. Interestingly, lipid-laden TG-EPM present significant differences in lysosome biology compared to BMDMs[91]. Therefore, some of the discrepancies could be additionally explained by a different mTORC1 response in peritoneal macrophages *vs*. the BMDMs used in their studies.

Atherosclerosis progression and plaque remodeling are determined by the crosstalk between vascular cells and macrophages in advanced plaques. In this regard, several chemokines and cytokines, among other bioactive molecules secreted by macrophages, influence the response of different cell types within the artery wall. Activated macrophages release 25-HC into the extracellular media[32,38,41,92,93], this in turn promotes paracrine effects in nearby cells, including alterations in membrane composition[38], migratory stimulation[93], or NFκB activation[92]. Our present study shows that in response to LPS, lipid-laden macrophages secrete 25-HC, without inducing the secretion of other oxysterols. This suggests that 25-HC has a predominant role under inflammatory conditions. Furthermore, 25-HC blunts SMC migration *in vitro* and reduces SMC content within the fibrous cap of WT→*Ldlr*$^{-/-}$ mice, suggesting that 25-HC could participate as a lipid mediator in the crosstalk among these two cell types. Mechanistically, we found that 25-HC alters PDGFRβ signaling in SMC *in vitro* by affecting the pool of PM free cholesterol which alters PDGFRβ location within high-cholesterol PM microdomains and subsequent signal events[80], which is in line with recent work that shows that SMCs that populate the fibrous cap in a PDGFRβ-dependent manner[94].

Our work emphasizes the pro-inflammatory role of macrophage-derived 25-HC and demonstrates that 25-HC promotes inflammation and atherogenesis. Mechanistically, our experiments showed that 25-HC produced by activated lipid-loaded macrophages boosts the inflammatory response, increases apoptosis sensitivity, reduces efferocytotic capacity and promotes paracrine effects in neighbor cells. Additionally, present results show that 25-HC is not a major regulator of LXR or SREBP2 transcriptional activity in lipid-laden activated

Author Manuscript Author Manuscript Author Manuscript Author Manuscript

macrophages. This work opens the door for future studies further exploring the role of 25-HC as a biomarker of inflammation and plaque stability in human atherosclerosis.

Supplementary Material

Refer to Web version on PubMed Central for supplementary material.

Acknowledgements

We thank Christopher Castaldi at Yale Center for Genome Analysis for RNA expression studies by bulk RNA-Seq and Rolando Garcia-Milian at Medical library for RNA-seq analysis advice. We also thank Dr. Jordan Pober at Yale School of Medicine for helpful suggestions. Working model graph was created with BioRender.com.

Source of Funding

The work at Suarez and Fernandez-Hernando laboratories is supported by grants from National Heart and Lung Institute (NHLBI), NIH (R35HL155988 to YS and R35HL135820 to CF-H) and the American Heart Association (AHA), (20TPA35490202 to YS and 20TPA35490416 to CFH). The collection of human coronary arteries was supported by R01 HL146723 to GT. Additional support is from R01 HL153712-01, NIH-NCATS UH3TR002067, AHA (20SFRN35210252) and CZI (NFL-2020-218415) to CG and 5F32DK10348902 to NLP. ACD and NR were recipient of grants from AHA (19POST34430108 to ACD and 17SDG33110002 to NR) and DG-C from Grant RTI2018-098113-B-I00 (Plan Estatal de Investigación Científica y Técnica y de Innovación 2017-2020, Ministerio de Ciencia, Innovación y Universidades, Spain, and the European Development Regional Fund (ERDF).

Non-standard Abbreviations and Acronyms

25-HC	25-hydroxycholesterol
CH25H	25-hydroxylase
BM	Bone marrow
WD	Western diet
SMC	Smooth muscle cell
TLR4	Toll-like receptor 4
NF-κB	Nuclear factor-κB
LXR	Liver X receptor
SREBP	Sterol regulatory-element binding protein
LDL	Low-density lipoproteins
Ox-LDL	Oxidized LDLs
HMG-CoA	Hydroxy methyl glutaryl-coenzyme A
LDLR	LDL receptor
ABC	ATP-binding cassette
IFN	Interferon
IL	Interleukin

Author Manuscript Author Manuscript Author Manuscript Author Manuscript

RNA-seq	RNA-sequencing
PM	Plasma membrane
LC/MS-MS	Liquid chromatography–mass spectrometry
scRNA-seq	Single cell RNA-seq
Apo E	Apolipoprotein E
SSC	Side Scatter
Cyp	Cytochrome P450 family
ORO	Oil red O
SMA	Smooth alpha actin
TG-EPM	Thioglycolate-elicited peritoneal macrophages
TFs	Transcription factors
ROS	Reactive oxygen species
LPS	Lipopolysaccharide
SMase	Sphingomyelinase
ALOD4	Anthrolysin O peptide
eGFP	Enhanced green fluorescence protein
BMDMs	BM derived macrophages

References

1. Cushing SD, Berliner JA, Valente AJ, Territo MC, Navab M, Parhami F, Gerrity R, Schwartz CJ, Fogelman AM. Minimally modified low density lipoprotein induces monocyte chemotactic protein 1 in human endothelial cells and smooth muscle cells. Proc Natl Acad Sci U S A. 1990;87:5134–5138. doi: 10.1073/pnas.87.13.5134 [PubMed: 1695010]
2. Hurt-Camejo E, Camejo G, Rosengren B, Lopez F, Ahlstrom C, Fager G, Bondjers G. Effect of arterial proteoglycans and glycosaminoglycans on low density lipoprotein oxidation and its uptake by human macrophages and arterial smooth muscle cells. Arterioscler Thromb. 1992;12:569–583. doi: 10.1161/01.atv.12.5.569 [PubMed: 1576119]
3. Skalen K, Gustafsson M, Rydberg EK, Hulten LM, Wiklund O, Innerarity TL, Boren J. Subendothelial retention of atherogenic lipoproteins in early atherosclerosis. Nature. 2002;417:750–754. doi: 10.1038/nature00804 [PubMed: 12066187]
4. Robbins CS, Hilgendorf I, Weber GF, Theurl I, Iwamoto Y, Figueiredo JL, Gorbatov R, Sukhova GK, Gerhardt LM, Smyth D, et al. Local proliferation dominates lesional macrophage accumulation in atherosclerosis. Nat Med. 2013;19:1166–1172. doi: 10.1038/nm.3258 [PubMed: 23933982]
5. Stewart CR, Stuart LM, Wilkinson K, van Gils JM, Deng J, Halle A, Rayner KJ, Boyer L, Zhong R, Frazier WA, et al. CD36 ligands promote sterile inflammation through assembly of a Toll-like receptor 4 and 6 heterodimer. Nat Immunol. 2010;11:155–161. doi: 10.1038/ni.1836 [PubMed: 20037584]
6. Sheedy FJ, Grebe A, Rayner KJ, Kalantari P, Ramkhelawon B, Carpenter SB, Becker CE, Ediriweera HN, Mullick AE, Golenbock DT, et al. CD36 coordinates NLRP3 inflammasome

Author Manuscript Author Manuscript Author Manuscript Author Manuscript

activation by facilitating intracellular nucleation of soluble ligands into particulate ligands in sterile inflammation. Nat Immunol. 2013;14:812–820. doi: 10.1038/ni.2639 [PubMed: 23812099]

7. Tabas I, Garcia-Cardena G, Owens GK. Recent insights into the cellular biology of atherosclerosis. J Cell Biol. 2015;209:13–22. doi: 10.1083/jcb.201412052 [PubMed: 25869663]
8. Moore KJ, Freeman MW. Scavenger receptors in atherosclerosis: beyond lipid uptake. Arterioscler Thromb Vasc Biol. 2006;26:1702–1711. doi: 10.1161/01.ATV.0000229218.97976.43 [PubMed: 16728653]
9. Medzhitov R, Janeway C Jr., Innate immune recognition: mechanisms and pathways. Immunol Rev. 2000;173:89–97. doi: 10.1034/j.1600-065x.2000.917309.x [PubMed: 10719670]
10. Kim K, Shim D, Lee JS, Zaitsev K, Williams JW, Kim KW, Jang MY, Seok Jang H, Yun TJ, Lee SH, et al. Transcriptome Analysis Reveals Nonfoamy Rather Than Foamy Plaque Macrophages Are Proinflammatory in Atherosclerotic Murine Models. Circ Res. 2018;123:1127–1142. doi: 10.1161/CIRCRESAHA.118.312804 [PubMed: 30359200]
11. Spann NJ, Glass CK. Sterols and oxysterols in immune cell function. Nat Immunol. 2013;14:893–900. doi: 10.1038/ni.2681 [PubMed: 23959186]
12. Back M, Yurdagul A Jr., Tabas I, Oorni K, Kovanen PT. Inflammation and its resolution in atherosclerosis: mediators and therapeutic opportunities. Nat Rev Cardiol. 2019;16:389–406. doi: 10.1038/s41569-019-0169-2 [PubMed: 30846875]
13. Janowski BA, Willy PJ, Devi TR, Falck JR, Mangelsdorf DJ. An oxysterol signalling pathway mediated by the nuclear receptor LXR alpha. Nature. 1996;383:728–731. doi: 10.1038/383728a0 [PubMed: 8878485]
14. Horton JD, Goldstein JL, Brown MS. SREBPs: activators of the complete program of cholesterol and fatty acid synthesis in the liver. J Clin Invest. 2002;109:1125–1131. doi: 10.1172/JCI15593 [PubMed: 11994399]
15. Joseph SB, Castrillo A, Laffitte BA, Mangelsdorf DJ, Tontonoz P. Reciprocal regulation of inflammation and lipid metabolism by liver X receptors. Nat Med. 2003;9:213–219. doi: 10.1038/nm820 [PubMed: 12524534]
16. Castrillo A, Joseph SB, Marathe C, Mangelsdorf DJ, Tontonoz P. Liver X receptor-dependent repression of matrix metalloproteinase-9 expression in macrophages. J Biol Chem. 2003;278:10443–10449. doi: 10.1074/jbc.M213071200 [PubMed: 12531895]
17. Ghisletti S, Huang W, Ogawa S, Pascual G, Lin ME, Willson TM, Rosenfeld MG, Glass CK. Parallel SUMOylation-dependent pathways mediate gene- and signal-specific transrepression by LXRs and PPARgamma. Mol Cell. 2007;25:57–70. doi: 10.1016/j.molcel.2006.11.022 [PubMed: 17218271]
18. Ghisletti S, Huang W, Jepsen K, Benner C, Hardiman G, Rosenfeld MG, Glass CK. Cooperative NCoR/SMRT interactions establish a corepressor-based strategy for integration of inflammatory and anti-inflammatory signaling pathways. Genes Dev. 2009;23:681–693. doi: 10.1101/gad.1773109 [PubMed: 19299558]
19. Oishi Y, Spann NJ, Link VM, Muse ED, Strid T, Edillor C, Kolar MJ, Matsuzaka T, Hayakawa S, Tao J, et al. SREBP1 Contributes to Resolution of Pro-inflammatory TLR4 Signaling by Reprogramming Fatty Acid Metabolism. Cell Metab. 2017;25:412–427. doi: 10.1016/j.cmet.2016.11.009 [PubMed: 28041958]
20. Guo C, Chi Z, Jiang D, Xu T, Yu W, Wang Z, Chen S, Zhang L, Liu Q, Guo X, et al. Cholesterol Homeostatic Regulator SCAP-SREBP2 Integrates NLRP3 Inflammasome Activation and Cholesterol Biosynthetic Signaling in Macrophages. Immunity. 2018;49:842–856 e847. doi: 10.1016/j.immuni.2018.08.021 [PubMed: 30366764]
21. Kusnadi A, Park SH, Yuan R, Pannellini T, Giannopoulou E, Oliver D, Lu T, Park-Min KH, Ivashkiv LB. The Cytokine TNF Promotes Transcription Factor SREBP Activity and Binding to Inflammatory Genes to Activate Macrophages and Limit Tissue Repair. Immunity. 2019;51:241–257 e249. doi: 10.1016/j.immuni.2019.06.005 [PubMed: 31303399]
22. Muse ED, Yu S, Edillor CR, Tao J, Spann NJ, Troutman TD, Seidman JS, Henke A, Roland JT, Ozeki KA, et al. Cell-specific discrimination of desmosterol and desmosterol mimetics confers selective regulation of LXR and SREBP in macrophages. Proc Natl Acad Sci U S A. 2018;115:E4680–E4689. doi: 10.1073/pnas.1714518115 [PubMed: 29632203]

Author Manuscript Author Manuscript Author Manuscript Author Manuscript

23. Adams CM, Reitz J, De Brabander JK, Feramisco JD, Li L, Brown MS, Goldstein JL. Cholesterol and 25-hydroxycholesterol inhibit activation of SREBPs by different mechanisms, both involving SCAP and Insigs. J Biol Chem. 2004;279:52772–52780. doi: 10.1074/jbc.M410302200 [PubMed: 15452130]
24. Zhang X, McDonald JG, Aryal B, Canfran-Duque A, Goldberg EL, Araldi E, Ding W, Fan Y, Thompson BM, Singh AK, et al. Desmosterol suppresses macrophage inflammasome activation and protects against vascular inflammation and atherosclerosis. Proc Natl Acad Sci U S A. 2021;118. doi: 10.1073/pnas.2107682118
25. Lund EG, Kerr TA, Sakai J, Li WP, Russell DW. cDNA cloning of mouse and human cholesterol 25-hydroxylases, polytopic membrane proteins that synthesize a potent oxysterol regulator of lipid metabolism. J Biol Chem. 1998;273:34316–34327. doi: 10.1074/jbc.273.51.34316 [PubMed: 9852097]
26. Radhakrishnan A, Ikeda Y, Kwon HJ, Brown MS, Goldstein JL. Sterol-regulated transport of SREBPs from endoplasmic reticulum to Golgi: oxysterols block transport by binding to Insig. Proc Natl Acad Sci U S A. 2007;104:6511–6518. doi: 10.1073/pnas.0700899104 [PubMed: 17428920]
27. Goldstein JL, DeBose-Boyd RA, Brown MS. Protein sensors for membrane sterols. Cell. 2006;124:35–46. doi: 10.1016/j.cell.2005.12.022 [PubMed: 16413480]
28. Yang C, McDonald JG, Patel A, Zhang Y, Umetani M, Xu F, Westover EJ, Covey DF, Mangelsdorf DJ, Cohen JC, et al. Sterol intermediates from cholesterol biosynthetic pathway as liver X receptor ligands. J Biol Chem. 2006;281:27816–27826. doi: 10.1074/jbc.M603781200 [PubMed: 16857673]
29. Chen W, Chen G, Head DL, Mangelsdorf DJ, Russell DW. Enzymatic reduction of oxysterols impairs LXR signaling in cultured cells and the livers of mice. Cell Metab. 2007;5:73–79. doi: 10.1016/j.cmet.2006.11.012 [PubMed: 17189208]
30. Venkateswaran A, Laffitte BA, Joseph SB, Mak PA, Wilpitz DC, Edwards PA, Tontonoz P. Control of cellular cholesterol efflux by the nuclear oxysterol receptor LXR alpha. Proc Natl Acad Sci U S A. 2000;97:12097–12102. doi: 10.1073/pnas.200367697 [PubMed: 11035776]
31. Du X, Pham YH, Brown AJ. Effects of 25-hydroxycholesterol on cholesterol esterification and sterol regulatory element-binding protein processing are dissociable: implications for cholesterol movement to the regulatory pool in the endoplasmic reticulum. J Biol Chem. 2004;279:47010–47016. doi: 10.1074/jbc.M408690200 [PubMed: 15317807]
32. Bauman DR, Bitmansour AD, McDonald JG, Thompson BM, Liang G, Russell DW. 25-Hydroxycholesterol secreted by macrophages in response to Toll-like receptor activation suppresses immunoglobulin A production. Proc Natl Acad Sci U S A. 2009;106:16764–16769. doi: 10.1073/pnas.0909142106 [PubMed: 19805370]
33. Russell DW. The enzymes, regulation, and genetics of bile acid synthesis. Annu Rev Biochem. 2003;72:137–174. doi: 10.1146/annurev.biochem.72.121801.161712 [PubMed: 12543708]
34. Bjorkhem I Are side-chain oxidized oxysterols regulators also in vivo? J Lipid Res. 2009;50 Suppl:S213–218. doi: 10.1194/jlr.R800025-JLR200 [PubMed: 18952574]
35. Diczfalusy U On the formation and possible biological role of 25-hydroxycholesterol. Biochimie. 2013;95:455–460. doi: 10.1016/j.biochi.2012.06.016 [PubMed: 22732193]
36. Araldi E, Fernandez-Fuertes M, Canfran-Duque A, Tang W, Cline GW, Madrigal-Matute J, Pober JS, Lasuncion MA, Wu D, Fernandez-Hernando C, et al. Lanosterol Modulates TLR4-Mediated Innate Immune Responses in Macrophages. Cell Rep. 2017;19:2743–2755. doi: 10.1016/j.celrep.2017.05.093 [PubMed: 28658622]
37. Blanc M, Hsieh WY, Robertson KA, Kropp KA, Forster T, Shui G, Lacaze P, Watterson S, Griffiths SJ, Spann NJ, et al. The transcription factor STAT-1 couples macrophage synthesis of 25-hydroxycholesterol to the interferon antiviral response. Immunity. 2013;38:106–118. doi: 10.1016/j.immuni.2012.11.004 [PubMed: 23273843]
38. Liu SY, Aliyari R, Chikere K, Li G, Marsden MD, Smith JK, Pernet O, Guo H, Nusbaum R, Zack JA, et al. Interferon-inducible cholesterol-25-hydroxylase broadly inhibits viral entry by production of 25-hydroxycholesterol. Immunity. 2013;38:92–105. doi: 10.1016/j.immuni.2012.11.005 [PubMed: 23273844]

Author Manuscript Author Manuscript Author Manuscript Author Manuscript

39. Li C, Deng YQ, Wang S, Ma F, Aliyari R, Huang XY, Zhang NN, Watanabe M, Dong HL, Liu P, et al. 25-Hydroxycholesterol Protects Host against Zika Virus Infection and Its Associated Microcephaly in a Mouse Model. Immunity. 2017;46:446–456. doi: 10.1016/j.immuni.2017.02.012 [PubMed: 28314593]
40. Liu Y, Wei Z, Zhang Y, Ma X, Chen Y, Yu M, Ma C, Li X, Cao Y, Liu J, et al. Activation of liver X receptor plays a central role in antiviral actions of 25-hydroxycholesterol. J Lipid Res. 2018;59:2287–2296. doi: 10.1194/jlr.M084558 [PubMed: 30309895]
41. Gold ES, Diercks AH, Podolsky I, Podyminogin RL, Askovich PS, Treuting PM, Aderem A. 25-Hydroxycholesterol acts as an amplifier of inflammatory signaling. Proc Natl Acad Sci U S A. 2014;111:10666–10671. doi: 10.1073/pnas.1404271111 [PubMed: 24994901]
42. Koarai A, Yanagisawa S, Sugiura H, Ichikawa T, Kikuchi T, Furukawa K, Akamatsu K, Hirano T, Nakanishi M, Matsunaga K, et al. 25-Hydroxycholesterol enhances cytokine release and Toll-like receptor 3 response in airway epithelial cells. Respir Res. 2012;13:63. doi: 10.1186/1465-9921-13-63 [PubMed: 22849850]
43. Reboldi A, Dang EV, McDonald JG, Liang G, Russell DW, Cyster JG. Inflammation. 25-Hydroxycholesterol suppresses interleukin-1-driven inflammation downstream of type I interferon. Science. 2014;345:679–684. doi: 10.1126/science.1254790 [PubMed: 25104388]
44. Dang EV, McDonald JG, Russell DW, Cyster JG. Oxysterol Restraint of Cholesterol Synthesis Prevents AIM2 Inflammasome Activation. Cell. 2017;171:1057–1071 e1011. doi: 10.1016/j.cell.2017.09.029 [PubMed: 29033131]
45. Li Z, Martin M, Zhang J, Huang HY, Bai L, Zhang J, Kang J, He M, Li J, Maurya MR, et al. Kruppel-Like Factor 4 Regulation of Cholesterol-25-Hydroxylase and Liver X Receptor Mitigates Atherosclerosis Susceptibility. Circulation. 2017;136:1315–1330. doi: 10.1161/CIRCULATIONAHA.117.027462 [PubMed: 28794002]
46. Gold ES, Ramsey SA, Sartain MJ, Selinummi J, Podolsky I, Rodriguez DJ, Moritz RL, Aderem A. ATF3 protects against atherosclerosis by suppressing 25-hydroxycholesterol-induced lipid body formation. J Exp Med. 2012;209:807–817. doi: 10.1084/jem.20111202 [PubMed: 22473958]
47. Chen PY, Qin L, Li G, Tellides G, Simons M. Smooth muscle FGF/TGFbeta cross talk regulates atherosclerosis progression. EMBO Mol Med. 2016;8:712–728. doi: 10.15252/emmm.201506181 [PubMed: 27189169]
48. Fernandez DM, Rahman AH, Fernandez NF, Chudnovskiy A, Amir ED, Amadori L, Khan NS, Wong CK, Shamailova R, Hill CA, et al. Single-cell immune landscape of human atherosclerotic plaques. Nat Med. 2019;25:1576–1588. doi: 10.1038/s41591-019-0590-4 [PubMed: 31591603]
49. Pan H, Xue C, Auerbach BJ, Fan J, Bashore AC, Cui J, Yang DY, Trignano SB, Liu W, Shi J, et al. Single-Cell Genomics Reveals a Novel Cell State During Smooth Muscle Cell Phenotypic Switching and Potential Therapeutic Targets for Atherosclerosis in Mouse and Human. Circulation. 2020;142:2060–2075. doi: 10.1161/CIRCULATIONAHA.120.048378 [PubMed: 32962412]
50. Spann NJ, Garmire LX, McDonald JG, Myers DS, Milne SB, Shibata N, Reichart D, Fox JN, Shaked I, Heudobler D, et al. Regulated accumulation of desmosterol integrates macrophage lipid metabolism and inflammatory responses. Cell. 2012;151:138–152. doi: 10.1016/j.cell.2012.06.054 [PubMed: 23021221]
51. Price NL, Rotllan N, Canfran-Duque A, Zhang X, Pati P, Arias N, Moen J, Mayr M, Ford DA, Baldan A, et al. Genetic Dissection of the Impact of miR-33a and miR-33b during the Progression of Atherosclerosis. Cell Rep. 2017;21:1317–1330. doi: 10.1016/j.celrep.2017.10.023 [PubMed: 29091769]
52. Li AC, Binder CJ, Gutierrez A, Brown KK, Plotkin CR, Pattison JW, Valledor AF, Davis RA, Willson TM, Witztum JL, et al. Differential inhibition of macrophage foam-cell formation and atherosclerosis in mice by PPARalpha, beta/delta, and gamma. J Clin Invest. 2004;114:1564–1576. doi: 10.1172/JCI18730 [PubMed: 15578089]
53. Diczfalusy U, Olofsson KE, Carlsson AM, Gong M, Golenbock DT, Rooyackers O, Flaring U, Bjorkbacka H. Marked upregulation of cholesterol 25-hydroxylase expression by lipopolysaccharide. J Lipid Res. 2009;50:2258–2264. doi: 10.1194/jlr.M900107-JLR200 [PubMed: 19502589]

Author Manuscript Author Manuscript Author Manuscript Author Manuscript

54. Park K, Scott AL. Cholesterol 25-hydroxylase production by dendritic cells and macrophages is regulated by type I interferons. J Leukoc Biol. 2010;88:1081–1087. doi: 10.1189/jlb.0610318 [PubMed: 20699362]
55. Tugal D, Liao X, Jain MK. Transcriptional control of macrophage polarization. Arterioscler Thromb Vasc Biol. 2013;33:1135–1144. doi: 10.1161/ATVBAHA.113.301453 [PubMed: 23640482]
56. Lang R, Patel D, Morris JJ, Rutschman RL, Murray PJ. Shaping gene expression in activated and resting primary macrophages by IL-10. J Immunol. 2002;169:2253–2263. doi: 10.4049/jimmunol.169.5.2253 [PubMed: 12193690]
57. Cuadrado A, Manda G, Hassan A, Alcaraz MJ, Barbas C, Daiber A, Ghezzi P, Leon R, Lopez MG, Oliva B, et al. Transcription Factor NRF2 as a Therapeutic Target for Chronic Diseases: A Systems Medicine Approach. Pharmacol Rev. 2018;70:348–383. doi: 10.1124/pr.117.014753 [PubMed: 29507103]
58. Kobayashi EH, Suzuki T, Funayama R, Nagashima T, Hayashi M, Sekine H, Tanaka N, Moriguchi T, Motohashi H, Nakayama K, et al. Nrf2 suppresses macrophage inflammatory response by blocking proinflammatory cytokine transcription. Nat Commun. 2016;7:11624. doi: 10.1038/ncomms11624 [PubMed: 27211851]
59. Chen B, Huang S, Su Y, Wu YJ, Hanna A, Brickshawana A, Graff J, Frangogiannis NG. Macrophage Smad3 Protects the Infarcted Heart, Stimulating Phagocytosis and Regulating Inflammation. Circ Res. 2019;125:55–70. doi: 10.1161/CIRCRESAHA.119.315069 [PubMed: 31092129]
60. Ramon-Vazquez A, de la Rosa JV, Tabraue C, Lopez F, Diaz-Chico BN, Bosca L, Tontonoz P, Alemany S, Castrillo A. Common and Differential Transcriptional Actions of Nuclear Receptors Liver X Receptors alpha and beta in Macrophages. Mol Cell Biol. 2019;39. doi: 10.1128/MCB.00376-18
61. Goedeke L, Canfran-Duque A, Rotllan N, Chaube B, Thompson BM, Lee RG, Cline GW, McDonald JG, Shulman GI, Lasuncion MA, et al. MMAB promotes negative feedback control of cholesterol homeostasis. Nat Commun. 2021;12:6448. doi: 10.1038/s41467-021-26787-7 [PubMed: 34750386]
62. Xaus J, Comalada M, Valledor AF, Lloberas J, Lopez-Soriano F, Argiles JM, Bogdan C, Celada A. LPS induces apoptosis in macrophages mostly through the autocrine production of TNF-alpha. Blood. 2000;95:3823–3831. [PubMed: 10845916]
63. Rayner KJ. Cell Death in the Vessel Wall: The Good, the Bad, the Ugly. Arterioscler Thromb Vasc Biol. 2017;37:e75–e81. doi: 10.1161/ATVBAHA.117.309229 [PubMed: 28637702]
64. Viaud M, Ivanov S, Vujic N, Duta-Mare M, Aira LE, Barouillet T, Garcia E, Orange F, Dugail I, Hainault I, et al. Lysosomal Cholesterol Hydrolysis Couples Efferocytosis to Anti-Inflammatory Oxysterol Production. Circ Res. 2018;122:1369–1384. doi: 10.1161/CIRCRESAHA.117.312333 [PubMed: 29523554]
65. Valledor AF, Hsu LC, Ogawa S, Sawka-Verhelle D, Karin M, Glass CK. Activation of liver X receptors and retinoid X receptors prevents bacterial-induced macrophage apoptosis. Proc Natl Acad Sci U S A. 2004;101:17813–17818. doi: 10.1073/pnas.0407749101 [PubMed: 15601766]
66. Joseph SB, Bradley MN, Castrillo A, Bruhn KW, Mak PA, Pei L, Hogenesch J, O'Connell RM, Cheng G, Saez E, et al. LXR-dependent gene expression is important for macrophage survival and the innate immune response. Cell. 2004;119:299–309. doi: 10.1016/j.cell.2004.09.032 [PubMed: 15479645]
67. Im SS, Osborne TF. Protection from bacterial-toxin-induced apoptosis in macrophages requires the lipogenic transcription factor sterol regulatory element binding protein 1a. Mol Cell Biol. 2012;32:2196–2202. doi: 10.1128/MCB.06294-11 [PubMed: 22493063]
68. Arai S, Shelton JM, Chen M, Bradley MN, Castrillo A, Bookout AL, Mak PA, Edwards PA, Mangelsdorf DJ, Tontonoz P, et al. A role for the apoptosis inhibitory factor AIM/Spalpha/Api6 in atherosclerosis development. Cell Metab. 2005;1:201–213. doi: 10.1016/j.cmet.2005.02.002 [PubMed: 16054063]
69. Schlegel M, Sharma M, Brown EJ, Newman AAC, Cyr Y, Afonso MS, Corr EM, Koelwyn GJ, van Solingen C, Guzman J, et al. Silencing Myeloid Netrin-1 Induces Inflammation Resolution

Author Manuscript Author Manuscript Author Manuscript Author Manuscript

and Plaque Regression. Circ Res. 2021;129:530–546. doi: 10.1161/CIRCRESAHA.121.319313 [PubMed: 34289717]

70. Aprahamian T, Rifkin I, Bonegio R, Hugel B, Freyssinet JM, Sato K, Castellot JJ Jr., Walsh K. Impaired clearance of apoptotic cells promotes synergy between atherogenesis and autoimmune disease. J Exp Med. 2004;199:1121–1131. doi: 10.1084/jem.20031557 [PubMed: 15096538]
71. Schrijvers DM, De Meyer GR, Kockx MM, Herman AG, Martinet W. Phagocytosis of apoptotic cells by macrophages is impaired in atherosclerosis. Arterioscler Thromb Vasc Biol. 2005;25:1256–1261. doi: 10.1161/01.ATV.0000166517.18801.a7 [PubMed: 15831805]
72. Thorp E, Cui D, Schrijvers DM, Kuriakose G, Tabas I. Mertk receptor mutation reduces efferocytosis efficiency and promotes apoptotic cell accumulation and plaque necrosis in atherosclerotic lesions of apoe−/− mice. Arterioscler Thromb Vasc Biol. 2008;28:1421–1428. doi: 10.1161/ATVBAHA.108.167197 [PubMed: 18451332]
73. Koseki M, Hirano K, Masuda D, Ikegami C, Tanaka M, Ota A, Sandoval JC, Nakagawa-Toyama Y, Sato SB, Kobayashi T, et al. Increased lipid rafts and accelerated lipopolysaccharide-induced tumor necrosis factor-alpha secretion in Abca1-deficient macrophages. J Lipid Res. 2007;48:299–306. doi: 10.1194/jlr.M600428-JLR200 [PubMed: 17079792]
74. Zhu X, Lee JY, Timmins JM, Brown JM, Boudyguina E, Mulya A, Gebre AK, Willingham MC, Hiltbold EM, Mishra N, et al. Increased cellular free cholesterol in macrophage-specific Abca1 knock-out mice enhances pro-inflammatory response of macrophages. J Biol Chem. 2008;283:22930–22941. doi: 10.1074/jbc.M801408200 [PubMed: 18552351]
75. Zhu X, Owen JS, Wilson MD, Li H, Griffiths GL, Thomas MJ, Hiltbold EM, Fessler MB, Parks JS. Macrophage ABCA1 reduces MyD88-dependent Toll-like receptor trafficking to lipid rafts by reduction of lipid raft cholesterol. J Lipid Res. 2010;51:3196–3206. doi: 10.1194/jlr.M006486 [PubMed: 20650929]
76. Yvan-Charvet L, Welch C, Pagler TA, Ranalletta M, Lamkanfi M, Han S, Ishibashi M, Li R, Wang N, Tall AR. Increased inflammatory gene expression in ABC transporter-deficient macrophages: free cholesterol accumulation, increased signaling via toll-like receptors, and neutrophil infiltration of atherosclerotic lesions. Circulation. 2008;118:1837–1847. doi: 10.1161/CIRCULATIONAHA.108.793869 [PubMed: 18852364]
77. Ito A, Hong C, Rong X, Zhu X, Tarling EJ, Hedde PN, Gratton E, Parks J, Tontonoz P. LXRs link metabolism to inflammation through Abca1-dependent regulation of membrane composition and TLR signaling. Elife. 2015;4:e08009. doi: 10.7554/eLife.08009 [PubMed: 26173179]
78. Zhou QD, Chi X, Lee MS, Hsieh WY, Mkrtchyan JJ, Feng AC, He C, York AG, Bui VL, Kronenberger EB, et al. Interferon-mediated reprogramming of membrane cholesterol to evade bacterial toxins. Nat Immunol. 2020;21:746–755. doi: 10.1038/s41590-020-0695-4 [PubMed: 32514064]
79. Abrams ME, Johnson KA, Perelman SS, Zhang LS, Endapally S, Mar KB, Thompson BM, McDonald JG, Schoggins JW, Radhakrishnan A, et al. Oxysterols provide innate immunity to bacterial infection by mobilizing cell surface accessible cholesterol. Nat Microbiol. 2020;5:929–942. doi: 10.1038/s41564-020-0701-5 [PubMed: 32284563]
80. Seong J, Huang M, Sim KM, Kim H, Wang Y. FRET-based Visualization of PDGF Receptor Activation at Membrane Microdomains. Sci Rep. 2017;7:1593. doi: 10.1038/s41598-017-01789-y [PubMed: 28487538]
81. Fernandez-Hernando C, Jozsef L, Jenkins D, Di Lorenzo A, Sessa WC. Absence of Akt1 reduces vascular smooth muscle cell migration and survival and induces features of plaque vulnerability and cardiac dysfunction during atherosclerosis. Arterioscler Thromb Vasc Biol. 2009;29:2033–2040. doi: 10.1161/ATVBAHA.109.196394 [PubMed: 19762778]
82. Shankman LS, Gomez D, Cherepanova OA, Salmon M, Alencar GF, Haskins RM, Swiatlowska P, Newman AA, Greene ES, Straub AC, et al. KLF4-dependent phenotypic modulation of smooth muscle cells has a key role in atherosclerotic plaque pathogenesis. Nat Med. 2015;21:628–637. doi: 10.1038/nm.3866 [PubMed: 25985364]
83. Russo L, Muir L, Geletka L, Delproposto J, Baker N, Flesher C, O'Rourke R, Lumeng CN. Cholesterol 25-hydroxylase (CH25H) as a promoter of adipose tissue inflammation in obesity and diabetes. Mol Metab. 2020;39:100983. doi: 10.1016/j.molmet.2020.100983 [PubMed: 32229247]

Author Manuscript Author Manuscript Author Manuscript Author Manuscript

84. Nagelin MH, Srinivasan S, Nadler JL, Hedrick CC. Murine 12/15-lipoxygenase regulates ATP-binding cassette transporter G1 protein degradation through p38- and JNK2-dependent pathways. J Biol Chem. 2009;284:31303–31314. doi: 10.1074/jbc.M109.028910 [PubMed: 19713213]
85. Madenspacher JH, Morrell ED, Gowdy KM, McDonald JG, Thompson BM, Muse G, Martinez J, Thomas S, Mikacenic C, Nick JA, et al. Cholesterol 25-hydroxylase promotes efferocytosis and resolution of lung inflammation. JCI Insight. 2020;5. doi: 10.1172/jci.insight.137189
86. Thorp E, Vaisar T, Subramanian M, Mautner L, Blobel C, Tabas I. Shedding of the Mer tyrosine kinase receptor is mediated by ADAM17 protein through a pathway involving reactive oxygen species, protein kinase Cdelta, and p38 mitogen-activated protein kinase (MAPK). J Biol Chem. 2011;286:33335–33344. doi: 10.1074/jbc.M111.263020 [PubMed: 21828049]
87. Tabas I. Macrophage death and defective inflammation resolution in atherosclerosis. Nat Rev Immunol. 2010;10:36–46. doi: 10.1038/nri2675 [PubMed: 19960040]
88. Sudhof TC, Van der Westhuyzen DR, Goldstein JL, Brown MS, Russell DW. Three direct repeats and a TATA-like sequence are required for regulated expression of the human low density lipoprotein receptor gene. J Biol Chem. 1987;262:10773–10779. [PubMed: 3611089]
89. Shibata N, Carlin AF, Spann NJ, Saijo K, Morello CS, McDonald JG, Romanoski CE, Maurya MR, Kaikkonen MU, Lam MT, et al. 25-Hydroxycholesterol activates the integrated stress response to reprogram transcription and translation in macrophages. J Biol Chem. 2013;288:35812–35823. doi: 10.1074/jbc.M113.519637 [PubMed: 24189069]
90. Bar-Peled L, Sabatini DM. Regulation of mTORC1 by amino acids. Trends Cell Biol. 2014;24:400–406. doi: 10.1016/j.tcb.2014.03.003 [PubMed: 24698685]
91. Weber K, Schilling JD. Distinct lysosome phenotypes influence inflammatory function in peritoneal and bone marrow-derived macrophages. Int J Inflam. 2014;2014:154936. doi: 10.1155/2014/154936 [PubMed: 25587484]
92. Pokharel SM, Shil NK, Gc JB, Colburn ZT, Tsai SY, Segovia JA, Chang TH, Bandyopadhyay S, Natesan S, Jones JCR, et al. Integrin activation by the lipid molecule 25-hydroxycholesterol induces a proinflammatory response. Nat Commun. 2019;10:1482. doi: 10.1038/s41467-019-09453-x [PubMed: 30931941]
93. Yi T, Wang X, Kelly LM, An J, Xu Y, Sailer AW, Gustafsson JA, Russell DW, Cyster JG. Oxysterol gradient generation by lymphoid stromal cells guides activated B cell movement during humoral responses. Immunity. 2012;37:535–548. doi: 10.1016/j.immuni.2012.06.015 [PubMed: 22999953]
94. Newman AAC, Serbulea V, Baylis RA, Shankman LS, Bradley X, Alencar GF, Owsiany K, Deaton RA, Karnewar S, Shamsuzzaman S, et al. Multiple cell types contribute to the atherosclerotic lesion fibrous cap by PDGFRbeta and bioenergetic mechanisms. Nat Metab. 2021;3:166–181. doi: 10.1038/s42255-020-00338-8 [PubMed: 33619382]
95. Rotllan N, Chamorro-Jorganes A, Araldi E, Wanschel AC, Aryal B, Aranda JF, Goedeke L, Salerno AG, Ramirez CM, Sessa WC, et al. Hematopoietic Akt2 deficiency attenuates the progression of atherosclerosis. FASEB J. 2015;29:597–610. doi: 10.1096/fj.14-262097 [PubMed: 25392271]
96. Canfran-Duque A, Rotllan N, Zhang X, Fernandez-Fuertes M, Ramirez-Hidalgo C, Araldi E, Daimiel L, Busto R, Fernandez-Hernando C, Suarez Y. Macrophage deficiency of miR-21 promotes apoptosis, plaque necrosis, and vascular inflammation during atherogenesis. EMBO Mol Med. 2017;9:1244–1262. doi: 10.15252/emmm.201607492 [PubMed: 28674080]
97. Zhang X, Sun J, Canfran-Duque A, Aryal B, Tellides G, Chang YJ, Suarez Y, Osborne TF, Fernandez-Hernando C. Deficiency of histone lysine methyltransferase SETDB2 in hematopoietic cells promotes vascular inflammation and accelerates atherosclerosis. JCI Insight. 2021;6. doi: 10.1172/jci.insight.147984
98. Seimon TA, Wang Y, Han S, Senokuchi T, Schrijvers DM, Kuriakose G, Tall AR, Tabas IA. Macrophage deficiency of p38alpha MAPK promotes apoptosis and plaque necrosis in advanced atherosclerotic lesions in mice. J Clin Invest. 2009;119:886–898. doi: 10.1172/JCI37262 [PubMed: 19287091]
99. Bligh EG, Dyer WJ. A rapid method of total lipid extraction and purification. Can J Biochem Physiol. 1959;37:911–917. doi: 10.1139/o59-099 [PubMed: 13671378]

Author Manuscript Author Manuscript Author Manuscript Author Manuscript

100. McDonald JG, Smith DD, Stiles AR, Russell DW. A comprehensive method for extraction and quantitative analysis of sterols and secosteroids from human plasma. J Lipid Res. 2012;53:1399–1409. doi: 10.1194/jlr.D022285 [PubMed: 22517925]
101. Mitsche MA, McDonald JG, Hobbs HH, Cohen JC. Flux analysis of cholesterol biosynthesis in vivo reveals multiple tissue and cell-type specific pathways. Elife. 2015;4:e07999. doi: 10.7554/eLife.07999 [PubMed: 26114596]
102. Endapally S, Infante RE, Radhakrishnan A. Monitoring and Modulating Intracellular Cholesterol Trafficking Using ALOD4, a Cholesterol-Binding Protein. Methods Mol Biol. 2019;1949:153–163. doi: 10.1007/978-1-4939-9136-5_12 [PubMed: 30790255]
103. Cochain C, Vafadarnejad E, Arampatzi P, Pelisek J, Winkels H, Ley K, Wolf D, Saliba AE, Zernecke A. Single-Cell RNA-Seq Reveals the Transcriptional Landscape and Heterogeneity of Aortic Macrophages in Murine Atherosclerosis. Circ Res. 2018;122:1661–1674. doi: 10.1161/CIRCRESAHA.117.312509 [PubMed: 29545365]
104. Willemsen L, de Winther MP. Macrophage subsets in atherosclerosis as defined by single-cell technologies. J Pathol. 2020;250:705–714. doi: 10.1002/path.5392 [PubMed: 32003464]
105. Do TH, Ma F, Andrade PR, Teles R, de Andrade Silva BJ, Hu C, Espinoza A, Hsu JE, Cho CS, Kim M, et al. TREM2 macrophages induced by human lipids drive inflammation in acne lesions. Sci Immunol. 2022;7:eabo2787. doi: 10.1126/sciimmunol.abo2787 [PubMed: 35867799]
106. El Kharbili M, Aviszus K, Sasse SK, Zhao X, Serban KA, Majka SM, Gerber AN, Gally F. Macrophage programming is regulated by a cooperative interaction between fatty acid binding protein 5 and peroxisome proliferator-activated receptor gamma. FASEB J. 2022;36:e22300. doi: 10.1096/fj.202200128R [PubMed: 35436029]
107. Guo Y, Liu Y, Zhao S, Xu W, Li Y, Zhao P, Wang D, Cheng H, Ke Y, Zhang X. Oxidative stress-induced FABP5 S-glutathionylation protects against acute lung injury by suppressing inflammation in macrophages. Nat Commun. 2021;12:7094. doi: 10.1038/s41467-021-27428-9 [PubMed: 34876574]
108. Seo J, Jeong DW, Park JW, Lee KW, Fukuda J, Chun YS. Fatty-acid-induced FABP5/HIF-1 reprograms lipid metabolism and enhances the proliferation of liver cancer cells. Commun Biol. 2020;3:638. doi: 10.1038/s42003-020-01367-5 [PubMed: 33128030]
109. Umbarawan Y, Enoura A, Ogura H, Sato T, Horikawa M, Ishii T, Sunaga H, Matsui H, Yokoyama T, Kawakami R, et al. FABP5 Is a Sensitive Marker for Lipid-Rich Macrophages in the Luminal Side of Atherosclerotic Lesions. Int Heart J. 2021;62:666–676. doi: 10.1536/ihj.20-676 [PubMed: 33994513]
110. Di Gregoli K, Somerville M, Bianco R, Thomas AC, Frankow A, Newby AC, George SJ, Jackson CL, Johnson JL. Galectin-3 Identifies a Subset of Macrophages With a Potential Beneficial Role in Atherosclerosis. Arterioscler Thromb Vasc Biol. 2020;40:1491–1509. doi: 10.1161/ATVBAHA.120.314252 [PubMed: 32295421]
111. Schneider WM, Chevillotte MD, Rice CM. Interferon-stimulated genes: a complex web of host defenses. Annu Rev Immunol. 2014;32:513–545. doi: 10.1146/annurev-immunol-032713-120231 [PubMed: 24555472]
112. Liu BC, Sarhan J, Panda A, Muendlein HI, Ilyukha V, Coers J, Yamamoto M, Isberg RR, Poltorak A. Constitutive Interferon Maintains GBP Expression Required for Release of Bacterial Components Upstream of Pyroptosis and Anti-DNA Responses. Cell Rep. 2018;24:155–168 e155. doi: 10.1016/j.celrep.2018.06.012 [PubMed: 29972777]
113. Goo YH, Son SH, Yechoor VK, Paul A. Transcriptional Profiling of Foam Cells Reveals Induction of Guanylate-Binding Proteins Following Western Diet Acceleration of Atherosclerosis in the Absence of Global Changes in Inflammation. J Am Heart Assoc. 2016;5:e002663. doi: 10.1161/JAHA.115.002663 [PubMed: 27091181]

Author Manuscript Author Manuscript Author Manuscript Author Manuscript

CLINICAL PERSPECTIVE

What is new?

- 25-hydroxycholesterol accumulates in human coronary atherosclerosis.
- 25-hydroxycholesterol produced by macrophages accelerates atherosclerosis progression and promotes plaque instability by promoting the inflammatory response in macrophages, and via paracrine actions on smooth muscle cells migratory response.
- 25-hydroxycholesterol in lipid-loaded macrophages amplifies their inflammatory response independently of the modulation of LXR or SREBP transcriptional activity.

What are the clinical implications?

- Inhibition of 25-hydroxycholesterol production might delay atherosclerosis progression and promotes plaque stability.
- Our study opens the door to explore the role of 25-hydroxycholesterol as a target to control inflammation and plaque stability in human atherosclerosis.

Author Manuscript Author Manuscript Author Manuscript Author Manuscript

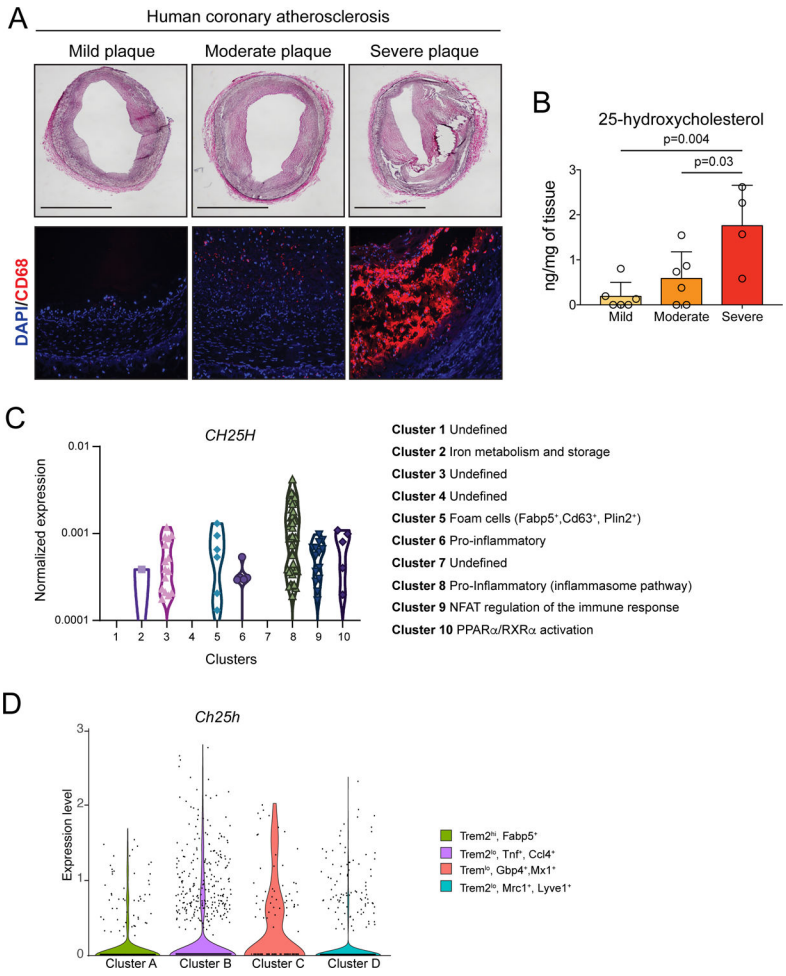

Figure 1. 25-hydroxycholesterol accumulates in human coronary atherosclerotic plaque and *CH25H* is highly express in human and mouse inflammatory plaque macrophages.

A, Representative hematoxylin, and eosin (H&E) staining (upper panels) and CD68 (macrophage marker) immunofluorescence (lower panels) of atherosclerotic plaques isolated from human coronary arteries. Scale bar: 1 mm. **B**, 25-hydroxycholesterol quantification in atherosclerotic plaques isolated from human coronary arteries. Data were analyzed by one-way ANOVA, post-hoc Bonferroni's multiple comparison test (n= 6 mild plaques, 6 moderate plaques and 4 severe plaques). **C**, Violin plots showing *CH25H* expression among different macrophages clusters presents in human plaque tissue[48]. **D**, Violin plot showing the expression of *Ch25h* withing the indicated macrophage clusters from leukocyte isolated from *Ldlr−/−* aortic tissue[10] of mice fed a WD for 12 weeks.

Author Manuscript Author Manuscript Author Manuscript Author Manuscript

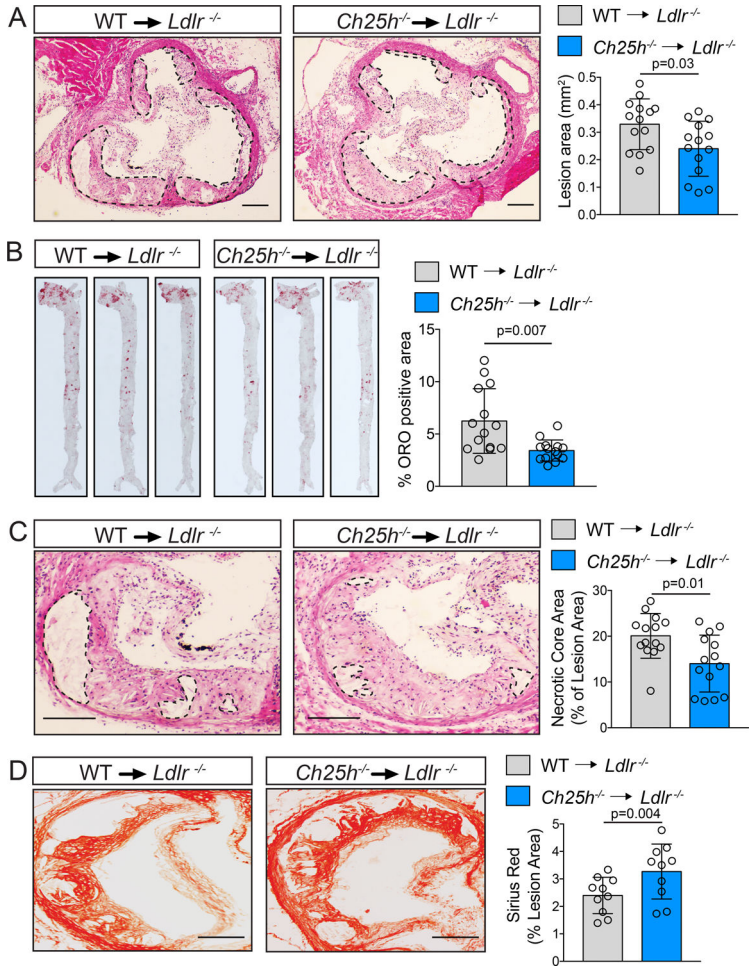

Figure 2. *Ch25h* deficiency in hematopoietic cells protects against atherosclerosis.

Analysis of *Ldlr*$^{-/-}$ mice transplanted with WT or *Ch25h*$^{-/-}$ bone marrow and fed for 12 weeks on a WD. **A, C**, Representative histological analysis of cross sections of the aortic sinus stained with hematoxylin and eosin (H&E). Dashed lines delimit the plaque area (**A**) and show the edge of the developing necrotic core (**C**). Quantification of plaque size (**A**) and necrotic core (**C**) are shown on the right panels (mean ±SD, n=14 mice per group). **B**, Representative *en face* ORO staining of aortas. Quantification of the ORO positive area is shown in the right panel and represents the mean ±SD (n=14 mice per group). **D**, Representative histological analysis of cross sections of the aortic sinus stained with Picrosirius Red. Quantification of the Picrosirius Red positive area is shown at the right panel and represents the mean ±SD (n=10 mice per group). All data were analyzed by Mann-Whitney non-parametric test. Scale bar: 100 μm.

Author Manuscript Author Manuscript Author Manuscript Author Manuscript

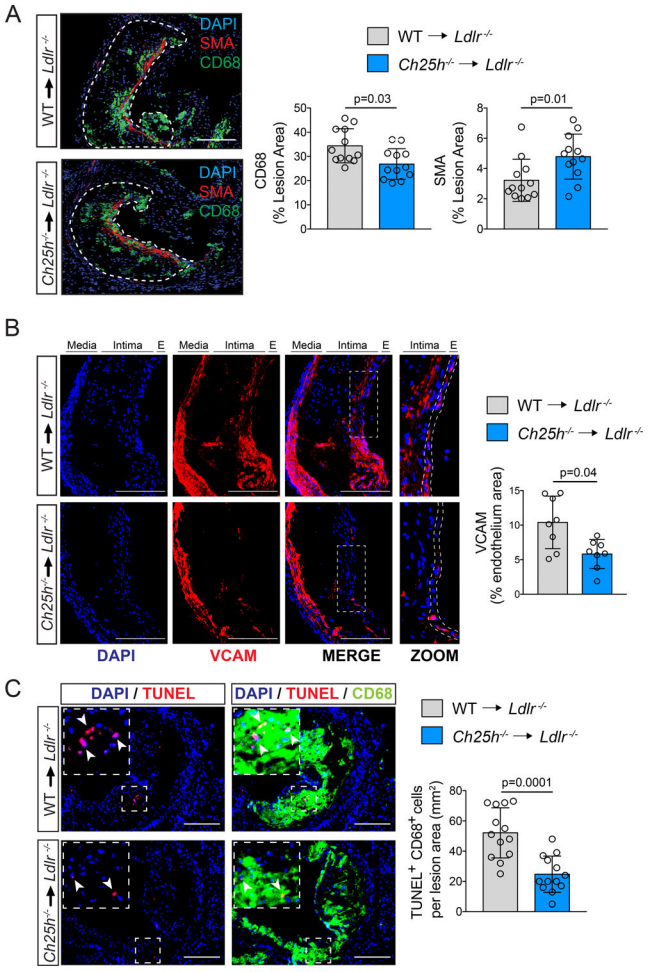

Figure 3. *Ch25h* deficiency in hematopoietic cells reduces vascular inflammation and promotes plaque stability.

Analysis of *Ldlr*$^{-/-}$ mice transplanted with WT or *Ch25h*$^{-/-}$ bone marrow and fed for 12 weeks on a WD**. A**, Representative histological analysis of cross sections of the aortic sinus stained with CD68 or smooth muscle actin (SMA). Dashed lines delimit the plaque area (**A**) Quantification of the CD68 or SMA positive area is shown on the right panels and represents the mean ±SD (n=12 mice per group). **B**, Representative histological analysis of cross sections of the aortic sinus stained with VCAM and DAPI. Quantification of the VCAM positive endothelium area is shown in the right panel and represents the mean ±SD (n=8 mice per group). In the enlarged images the dashed lines show how the endothelium area was delimited for quantification. **C**, Representative histological analysis of cross sections of the aortic sinus stained with CD68 and TUNEL. Quantification of the CD68-positive cells with TUNEL-positive nuclei is shown in the right panel and represents the mean ±SD (n=13 mice per group). DAPI was used to stain the nuclei. All data were analyzed by Mann-Whitney non-parametric test. Scale bar: 100 μm.

Author Manuscript Author Manuscript Author Manuscript Author Manuscript

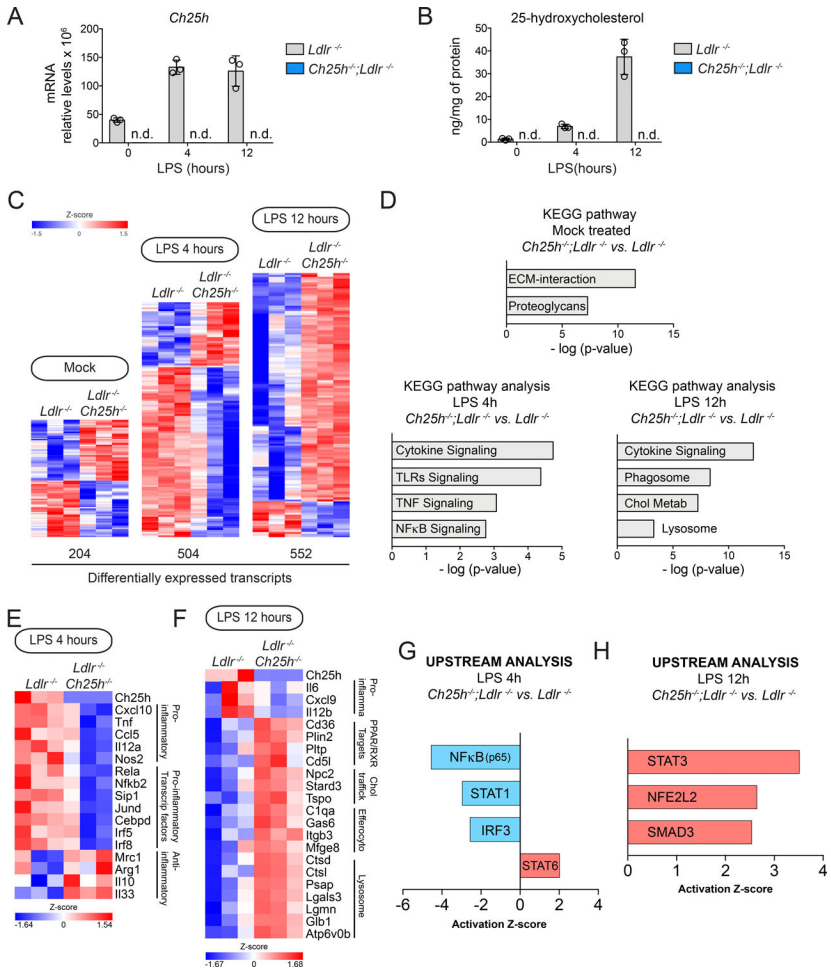

Figure 4. 25-hydroxycholesterol in lipid-laden macrophages promotes an inflammatory gene expression profile.

Analysis of lipid-laden TG-EPM isolated from *Ldlr*$^{-/-}$ or *Ch25h*$^{-/-}$;*Ldlr*$^{-/-}$ mice (n=3 mice per genotype), treated with LPS (100 ng/ml) for 4 or 12 hours. **A**, *Ch25h* relative mRNA expression levels in where n.d. means not detected **B**, LC/MS-MS quantification of 25-hydroxycholesterol, in where n.d. means not detected. **C**, Heatmaps of differentially expressed genes. A default *P*-value ≤ 0.05 was considered statistically significant with a fold-change ≥ 1.5 for up-regulated transcripts or ≤ −1.5 for down-regulated transcripts. **D**, Kyoto Encyclopedia of Gene and Genomes (KEGG) pathway enrichment analysis of differentially expressed genes at different time points. **E** & **F**, Heatmaps of representative genes differentially expressed involved in inflammation and resolution of inflammation. A default *P*-value ≤ 0.05 was considered statistically significant with a fold-change ≥ 1.5 for up-regulated transcripts or ≤ −1.5 for down-regulated transcripts. **G** & **H**, Upstream analysis using Ingenuity Pathway Analysis Software of Transcription factors in the above indicated macrophages treated with 100ng/ml LPS for 4 hours (**G**) or 12 hours (**H**). Transcription factors predicted to be activated (z-score > 0) appear in red and those that were predicted to be inactive (z-score < 0) appear in blue.

Author Manuscript Author Manuscript Author Manuscript Author Manuscript

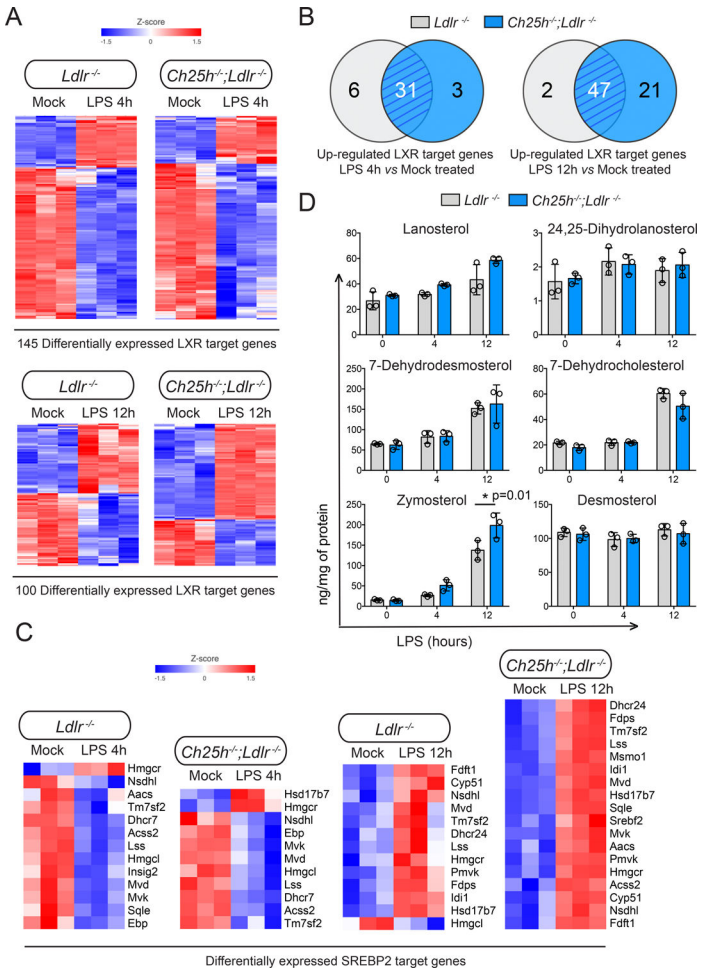

Figure 5. 25-hydroxycholesterol in lipid-laden macrophages is not necessary for LXR or SREBP transcriptional regulation.

Analysis of lipid-laden TG-EPM isolated from *Ldlr*$^{-/-}$ or *Ch25h*$^{-/-}$;*Ldlr*$^{-/-}$ mice (n=3 mice per genotype), treated with LPS (100 ng/ml) for 4 or 12 hours. **A**, Heatmaps showing LXR target genes differentially expressed in response to LPS treatment for 4 or 12 hours respectively. A default *P*-value ≤ 0.05 was considered statistically significant with a fold-change ≥ 1.5 for up-regulated transcripts or ≤ −1.5 for down-regulated transcripts. **B**, Venn diagrams depicting the overlap of upregulated LXR target genes. **C**, Heatmaps illustrating the effect of LPS treatment for 4 or 12 hours on SREBP2. A default *P*-value ≤ 0.05 was considered statistically significant with a fold-change ≥ 1.5 for up-regulated transcripts or ≤ −1.5 for down-regulated transcripts. **D**, Lipidomic analysis of sterol biosynthetic intermediates in macrophages isolated and treated as above. Data were analyzed by two-way ANOVA, post-hoc Bonferroni's multiple comparison test (n=3 mice per genotype).

Author Manuscript Author Manuscript Author Manuscript Author Manuscript

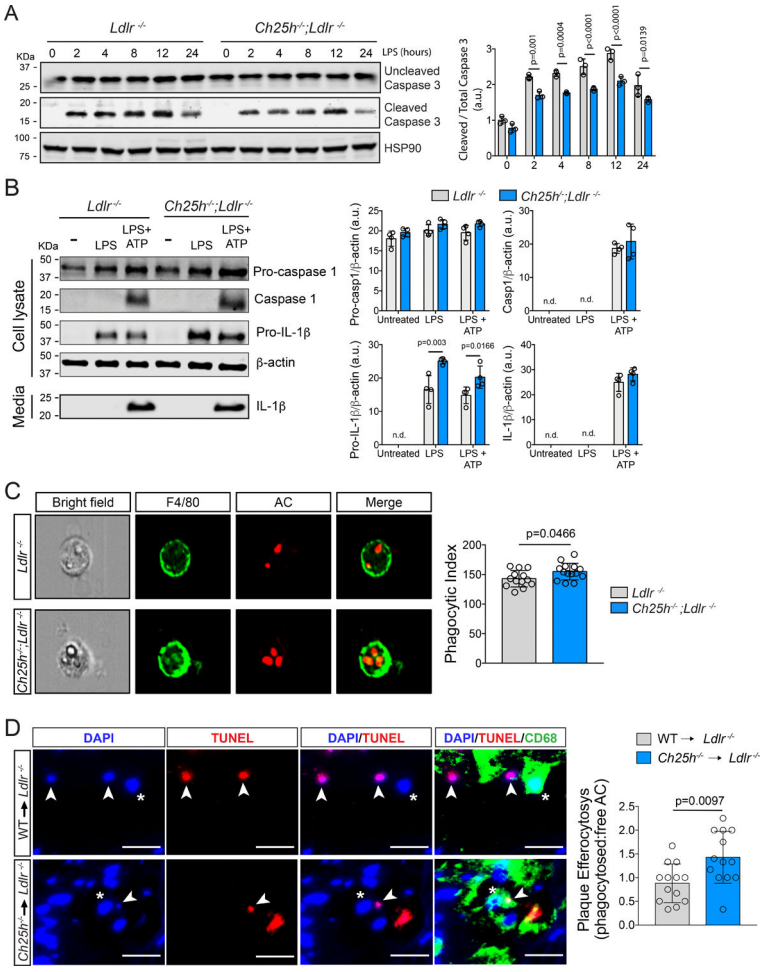

Figure 6. *Ch25h* deficiency in macrophage reduces LPS-induced apoptosis independently of inflammasome activation but increases macrophages efferocytotic activity.

A, Representative Western blot analysis of cleaved and total caspase-3 in *Ldlr*$^{-/-}$ or *Ch25h*$^{-/-}$;*Ldlr*$^{-/-}$ lipid-laden TG-EPM treated with LPS (100 ng/ml) at the indicated times. HSP90 was used as a loading control. Relative protein quantification by band densitometry is shown in the right panel. Data were analyzed by two-way ANOVA, post-hoc Bonferroni's multiple comparison test (n=3). n.d, not detectable. **B**, Representative Western blot analysis of caspase-1 and IL-1β as a read out of inflammasome activation of *Ldlr*$^{-/-}$ or *Ch25h*$^{-/-}$;*Ldlr*$^{-/-}$ lipid-laden TG-EPM with LPS (100 ng/ml) for 8 hours. ATP (5 mM) was added the last 30 minutes and prior to samples collection. Relative protein quantification by band densitometry is shown in the right panels. β-Actin was used as a loading control. Data were analyzed by two-way ANOVA, post-hoc Bonferroni's multiple comparison test (n=3). n.d. not detectable. **C**, Representative images of the *in vitro* engulfment of CellTracker Deep Red labeled apoptotic Jurkat cells by lipid-laden TG-EPM from Ldlr$^{-/-}$ or *Ch25h*$^{-/-}$;*Ldlr*$^{-/-}$ mice (n=14 mice per group). Data were acquired by Amnis Imagestream-X MarkII Imaging Flow Cytometer. Right panel shows efferocytosis quantification as phagocytic index, which is the number of apoptotic cells (red) ingested in 1 h per F4/80-positive macrophage (green) × 100. Significance was determined by Mann-Whitney non-parametric test. **D**, Representative images of the *in situ* efferocytosis assay. Apoptotic bodies were identified

as TUNEL-positive nuclei (white arrow heads) and macrophages as CD68 positive cells (asteriscs). Free apoptotic bodies were those TUNEL-positive nuclei that do not overlap with CD68 (upper panels), whereas TUNEL-positive nuclei that do overlap with CD68 (lower panels) are considered phagocytosed apoptotic bodies. Right panel shows the quantification of the phagocytosed versus free apoptotic bodies ratio (n= 13 mice per group). Data were analyzed by Mann-Whitney non-parametric test. Scale bar: 10 μm.

Author Manuscript Author Manuscript Author Manuscript Author Manuscript

Author Manuscript Author Manuscript Author Manuscript Author Manuscript

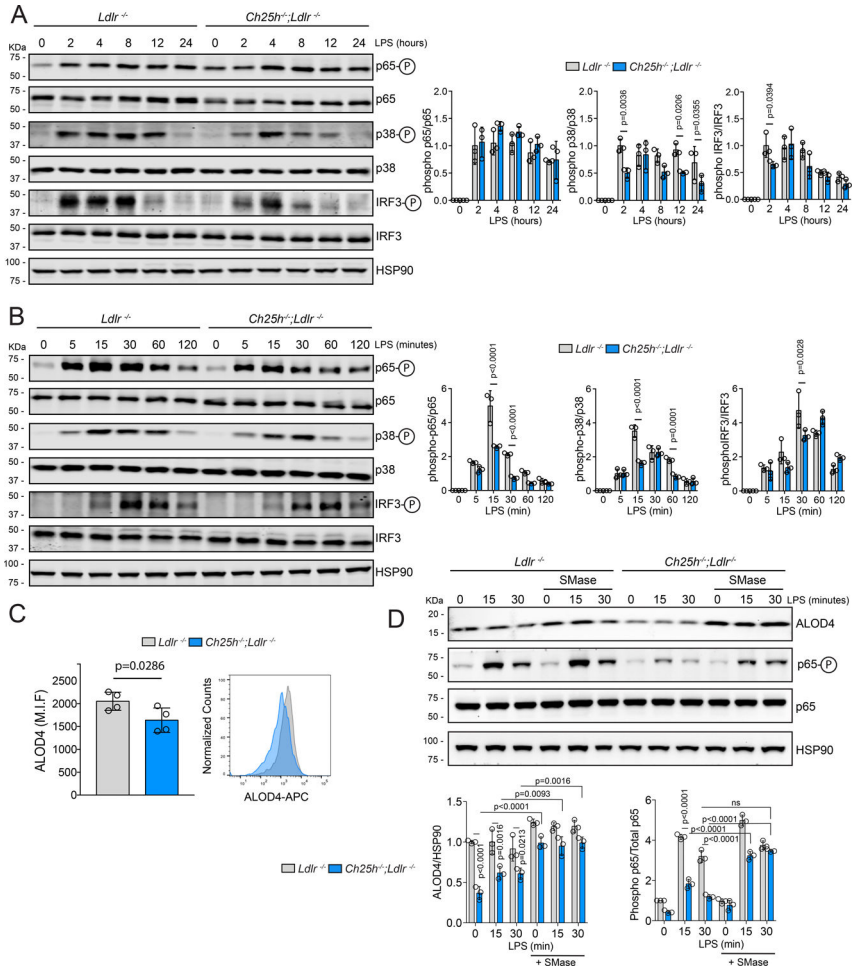

Figure 7. 25-hydroxycholesterol alters TLR4 downstream signaling by reducing the accessible cholesterol in the plasma membrane.

A-B, Representative Western blot of phospho-p65, p65, phospho-p38, p38, phospho-IRF3, IRF3 or HSP90 in *Ldlr*$^{-/-}$ or *Ch25h*$^{-/-}$*;Ldlr*$^{-/-}$ lipid-laden TG-EPM treated with LPS (100 ng/ml) at the indicated time points. HSP90 was used as loading control. Quantification of the relative phosphorylation is showing at the right panels. Data were analyzed by two-way ANOVA, post-hoc Bonferroni's multiple comparison test (n=3). **C**, Quantification of ALOD4 PM binding, in lipid-laden TG-EPM from *Ldlr*$^{-/-}$ or *Ch25h*$^{-/-}$*;Ldlr*$^{-/-}$ mice, by flow cytometry. Representative histogram is showing in the bottom panel. Data are average of the mean of Median Intensity Fluorescence (M.I.F.) in arbitrary units (a.u.) and analyzed by Mann-Whitney non-parametric test (n=4). **D**, Representative Western blot of phospho-p65, p65, ALOD4 or HSP90 in lipid-laden TG-EPM from *Ldlr*$^{-/-}$ or *Ch25h*$^{-/-}$*;Ldlr*$^{-/-}$ treated with LPS (100 ng/ml) in the presence or absence of Sphingomyelinase (200 mU/ml) at the indicated time points. Quantification of ALOD4 and the relative p65 phosphorylation is showed in the right panel. HSP90 was used as loading control. Data were analyzed by two-way ANOVA, post-hoc Bonferroni's multiple comparison test (n=3).

Author Manuscript Author Manuscript Author Manuscript Author Manuscript

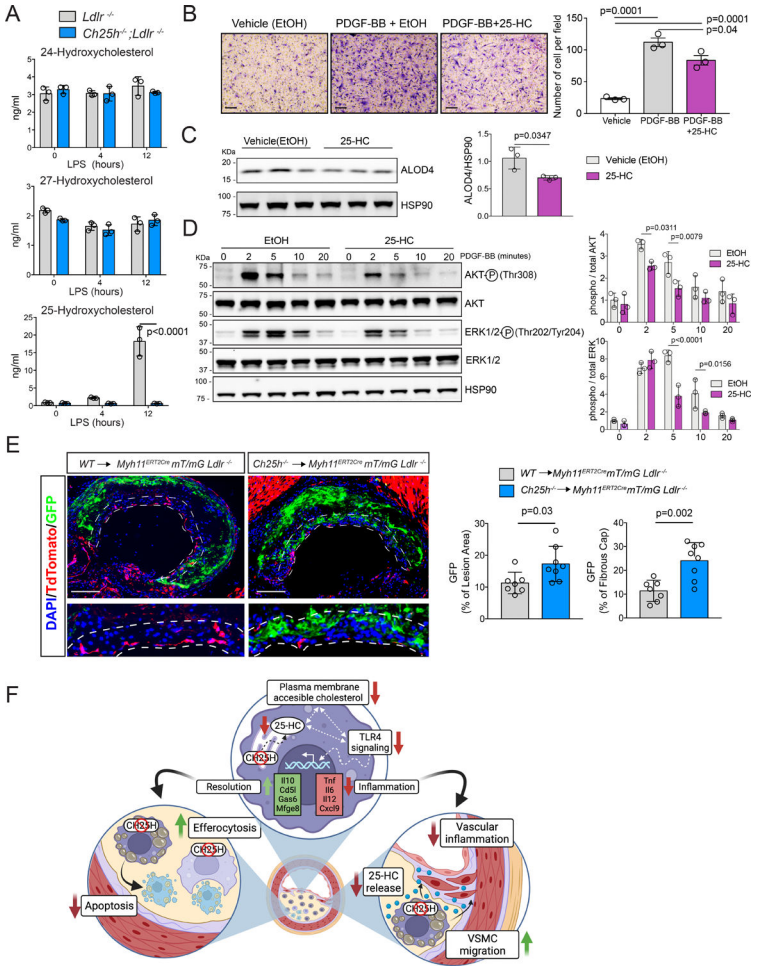

Figure 8. 25-hydroxycholesterol secreted by macrophages inhibits vascular smooth muscle cells migration.

A, LC/MS-MS quantification of several oxysterols presents in the media of cultured lipid-laden TG-EPM from *Ldlr*$^{-/-}$ or *Ch25h*$^{-/-}$;*Ldlr*$^{-/-}$ (n=3 mice per genotype) treated with LPS (100 ng/ml) for 4 or 12 hours. Data were analyzed by two-way ANOVA, post-hoc Bonferroni's multiple comparison test. **B**, SMC migration in the presence of PDGF-BB (10 ng/ml) or PDGF-BB plus 25-HC (5μM). 5 images were taken randomly per trans-well. Quantification is showing in the right panel and represent the mean ±SEM of 3 independent experiments. Data were analyzed by one-way ANOVA, post-hoc Bonferroni's multiple comparison test. Scale bar: 100 μm. **C**, Western blot analysis of ALOD4 binding into the PM in SMC treated with ethanol (EtOH) or 25-hydroxycholesterol (25-HC) at a concentration of 5μM for 2 hours. Quantification of ALOD4 is showed in the right panel. Data were analyzed by Mann-Whitney non-parametric test. **D**, Representative Western blot of phospho-AKT, AKT, phospho-ERK1/2, ERK1/2 or HSP90 in SMC pre-treated with EtOH or 25-HC (5μM) for 2 hours and then stimulated with PDGF-BB (10 ng/ml) for the indicated times. Quantification of the relative AKT and ERK1/2 phosphorylation is showed in the right panel. Data were analyzed by two-way ANOVA, post-hoc Bonferroni's multiple comparison test (n=3). **E**, Representative histological analysis of cross sections of the aortic sinus stained with eGFP and Tdtomato of *Myh11*^{CRE};*mT/mG; Ldlr*$^{-/-}$ mice

Author Manuscript Author Manuscript Author Manuscript Author Manuscript

transplanted with bone marrow from *WT* or *Ch25h*$^{-/-}$ donor mice and fed for 12 weeks a WD. Dashed lines define the fibrous cap area used for quantification. Scale bar: 100 μm. Quantification of the eGFP positive area within the whole plaque or the fibrous cap are shown at the right panels and represents the mean ±SD (n=8 mice per group) DAPI was used to stain the cell nucleus. All data were analyzed by Mann-Whitney non-parametric test. **F**, Proposed working model of 25-HC in macrophages in the context of atherosclerosis. Macrophages-derived 25-HC accelerates atherosclerosis progression and promotes plaque instability. Mechanistically we found that lack of 25-HC synthesis favors a reduction of accessible cholesterol in the PM, what diminishes pro-inflammatory response initiated by pattern recognition receptors in lipid-laden macrophages and promotes a reprogramming into a more pro-resolving phenotype (up). This pro-resolving phenotype is characterized by a better efferocytotic capacity and a lower susceptibility to stress-associated apoptosis in hypercholesterolemic macrophages *Ch25h* deficient (right). Additionally, the lack of macrophage-derived 25-HC released allows the migration of tunica media smooth muscle cells into the intima to form the fibrous cap (left).